Integrated Ocean Drilling Program
Expedition 310 Preliminary Report

Tahiti Sea Level

The last deglacial sea level rise in the South Pacific: offshore drilling in Tahiti (French Polynesia)

Cruise dates:
6 October–16 November 2005

Onshore Science Party:
13 February–4 March 2006

Expedition 310 Scientists

PUBLISHER'S NOTES

Citation:
Expedition 310 Scientists, 2006. Tahiti Sea Level: the last deglacial sea level rise in the South Pacific: offshore drilling in Tahiti (French Polynesia). IODP Prel. Rept. , 310. doi:10.2204/iodp.pr.310.2006

Distribution:
Electronic copies of this series may be obtained from the ECORD Web site on the World Wide Web at ecord.org/exp/pubs.html.

This publication was prepared by the Integrated Ocean Drilling Program ECORD Science Operator, as an account of work performed under the international Integrated Ocean Drilling Program, which is managed by IODP Management International (IODP-MI), Inc. Funding for the program is provided by the following agencies:

European Consortium for Ocean Research Drilling (ECORD)

Ministry of Education, Culture, Sports, Science and Technology (MEXT) of Japan

Ministry of Science and Technology (MOST), People's Republic of China

U.S. National Science Foundation (NSF)

DISCLAIMER

May 26, 2006

The following scientists and personnel participated in Expedition 310 of the Integrated Ocean Drilling Program.

EXPEDITION 310 PARTICIPANTS

Expedition 310 Scientists

Gilbert F. Camoin†
Co-Chief Scientist
Europôle Méditerranéen de l'Arbois
Centre Européen de Recherche et d'Enseignement des Geosciences de l'Environnement
Centre National de la Recherche Scientifique
UMR 6635
BP 80
13545 Aix-en-Provence Cedex 4
France
gcamoin@cerege.fr

Yasufumi Iryu†
Co-Chief Scientist
Institute of Geology and Paleontology
Graduate School of Science
Tohoku University
Aobayama
Sendai 980-8578
Japan
iryu@dges.tohoku.ac.jp

David McInroy†
Staff Scientist
British Geological Survey
Murchison House
West Mains Road
Edinburgh EH9 3LA
United Kingdom
dbm@bgs.ac.uk

Ryuji Asami
Inorganic Geochemist
Institute of Geology and Paleontology
Graduate School of Science
Tohoku University
Aobayama
Sendai 980-8578
Japan
ryuji@dges.tohoku.ac.jp

Hendrik Braaksma†
Petrophysics Staff Scientist
Laboratoire de Géophysique et Hydrodynamique en Forage
Université Montpellier II
ISTEEM 056 - Place Eugène Bataillon
34095 Montpellier Cedex 5
France
hendrik.braaksma@dstu.univ-montp2.fr

Guy Cabioch
Carbonate Sedimentologist
Research Unit "Paleotropique"
Institut de Recherche pour le Développement
BP A5
98848 Nouméa Cedex
New Caledonia
France
cabioch@noumea.ird.nc

Paterno Castillo
Igneous Petrologist
Scripps Institution of Oceanography
University of California, San Diego
9500 Gilman Drive
La Jolla CA 92093-0212
USA
pcastillo@ucsd.edu

Anne L. Cohen
Inorganic Geochemist
Geology and Geophysics
Woods Hole Oceanographic Institution
Clark 118
Mailstop 23
Woods Hole MA 02543
USA
acohen@whoi.edu

Julia E. Cole
Inorganic Geochemist
Geosciences Department
University of Arizona
1040 East 4th Street
Tucson AZ 85721
USA
jcole@geo.arizona.edu

†Participated in shipboard operations.

Pierre Deschamps
Inorganic Geochemist
Europole Mediterraneen de l'Arbois
Centre Européen de Recherche et d'Enseignement des Geosciences de l'Environnement
Centre National de la Recherche Scientifique
UMR 6635
BP 80
13545 Aix-en-Provence Cedex 4
France
deschamps@cerege.fr

Richard G. Fairbanks
Inorganic Geochemist
Earth and Environmental Sciences
Lamont-Doherty Earth Observatory of Columbia University
210 Isotope Laboratory
PO Box 1000, 61 Route 9W
Palisades NY 10964
USA
fairbanks@ldeo.columbia.edu

Thomas Felis
Inorganic Geochemist
Deutsche Forschungsgemeinschaft–Research Center Ocean Margins
University of Bremen
Postfach 330440
28334 Bremen
Germany
tfelis@uni-bremen.de

Kazuhiko Fujita
Paleontologist (foraminifers)
Department of Physics and Earth Sciences
University of the Ryukyus
Senbaru 1, Nishihara-cho
Okinawa 903-01
Japan
fujitaka@sci.u-ryukyu.ac.jp

Ed C. Hathorne
Inorganic Geochemist
Department of Earth Sciences
The Open University
Walton Hall
Milton Keynes MK7 6AA
United Kingdom
E.C.Hathorne@open.ac.uk

Steve P. Lund
Paleomagnetist
Department of Earth Sciences
University of Southern California
3651 University Avenue
Los Angeles CA 90089-0740
USA
slund@usc.edu

Hideaki Machiyama
Core Petrophysicist
Kochi Institute for Core Sample Research
Japan Agency for Marine-Earth Science and Technology (JAMSTEC)
200 Monobe-otsu, Nankoku
Kochi 783-8502
Japan
bucci@jamstec.go.jp

Hiroki Matsuda†
Carbonate Sedimentologist
Department of Earth Sciences, Faculty of Science
Kumamoto University
2-39-1, Kurokami
Kumamoto 860-8555
Japan
hmat@sci.kumamoto-u.ac.jp

Terrence M. Quinn
Inorganic Geochemist
College of Marine Science
University of South Florida
140 7th Avenue South
MSL 119
St. Petersburg FL 33711
USA
quinn@marine.usf.edu

Kaoru Sugihara†
Coral Specialist
Earth System Science, Faculty of Science
Fukuoka University
8-19-1, Nanakuma
Jonan-ku, Fukuoka
814-0180
Japan
sugihara@fukuoka-u.ac.jp

Alexander Thomas
Inorganic Geochemist
Department of Earth Science
University of Oxford
Parks Road
Oxford OX1 3PR
United Kingdom
alext@earth.ox.ac.uk

Crisogono de Olivera Vasconcelos†
Microbiologist
Department of Earth Sciences, Geological Institute
Swiss Federal Institute of Technology
Universität Strasse 6
8092 Zürich
Switzerland
Cris.Vasconcelos@erdw.ethz.ch

Klaas Verwer†
Core Petrophysicist/Logging Scientist
Faculty of Earth and Life Sciences
Department of Sedimentology and Marine Geology
Vrije Universiteit
de Boelelaan 1085
1081 Amsterdam
The Netherlands
klaas.verwer@falw.vu.nl

Jody M. Webster†
Coral Specialist
School of Earth Sciences
James Cook University of North Queensland
Townsville QLD 4811
Australia
Jody.Webster@jcu.edu.au

Hildegard Westphal
Carbonate Sedimentologist
Department of Geosciences
Universität Bremen
Leobener Strasse
28359 Bremen
Germany
hildegard.westphal@uni-bremen.de

Kyung Sik Woo
Carbonate Sedimentologist (observer)
Department of Geology
Kangwon National University
192-1, Hyoja2-Dong
Chunchon
Kangwon-Do 200-701
Korea
wooks@kangwon.ac.kr

Tsutomu Yamada†
Carbonate Sedimentologist
Institute of Geology and Paleontology
Graduate School of Science
Tohoku University
Aobayama
Sendai 980-8578
Japan
yamada@dges.tohoku.ac.jp

Yusuke Yokoyama
Inorganic Geochemist
Department of Earth and Planetary Sciences
University of Tokyo
7-3-1 Hongo
Building 1
Tokyo 113-0033
Japan
yokoyama@eps.s.u-tokyo.ac.jp

Operational and Technical Staff

ECORD Science Operator Personnel and Technical Representatives

Alister Skinner†
Operations Manager
British Geological Survey
Marine Operations
Engineering and Core Store
2a Nivensknowe Road
Loanhead EH20 9AU
United Kingdom
acsk@bgs.ac.uk

Ursula Röhl
Laboratory and Curation Manager
Bremen Core Repository (BCR)
Institute for Marine Environmental Research (MARUM)
Universität Bremen
Leobener Strasse
28359 Bremen
Germany
uroehl@marum.de

Davie Baxter†
Drilling Supervisor/Engineer
British Geological Survey
Marine Operations
Engineering and Core Store
2a Nivensknowe Road
Loanhead EH20 9AU
United Kingdom
dhba@bgs.ac.uk

Peter Bouteloup
Core Technician
British Geological Survey
Kingsley Dunham Centre
Keyworth
Nottingham HG12 5GG
United Kingdom
pbb@bgs.ac.uk

Florence Einaudi†
Logging Services
Laboratoire de Géophysique et d'Hydrodynamique en Forage
Université Montpellier II
ISTEEM 056
34095 Montpellier Cedex 5
France
florence.einaudi@dstu.univ-montp2.fr

Eileen Gillespe†
Drilling Engineer/Yeoperson
British Geological Survey
Murchison House
West Mains Road
Edinburgh EH9 3LA
United Kingdom
ejg@bgs.ac.uk

Colin Graham
Database Operator
British Geological Survey
Murchison House
West Mains Road
Edinburgh EH9 3LA
United Kingdom
ccg@bgs.ac.uk

Walter Hale
Core Curator
Bremen Core Repository (BCR)
Institute for Marine Environmental Research (MARUM)
Universität Bremen
Leobener Strasse
28359 Bremen
Germany
whale@uni-bremen.de

Gilles Henry†
Logging Services
Laboratoire de Géophysique et Hydrodynamique en Forage
Université Montpellier II
ISTEEM 056 - Place Eugène Bataillon
34095 Montpellier Cedex 5
France
gilles.henry@dstu.univ-montp2.fr

Jenny Inwood†
ESO Petrophysicist
Leicester University Borehole Research
Geology Department
Leicester University
University Road
Leicester LE1 7RH
United Kingdom
ji18@le.ac.uk

Martin Kölling†
ESO Geochemist
Department of Geosciences
University of Bremen
FB 5, Postfach 330440
28334 Bremen
Germany

Holger Kuhlmann†
Core Curator†**/Assistant Laboratory Manager**
Bremen Core Repository (BCR)
Institute for Marine Environmental Research (MARUM)
Universität Bremen
Leobener Strasse
28359 Bremen
Germany
hujlma@marum.de

Iain Pheasant†
Drilling Supervisor/Engineer
British Geological Survey
Marine Operations
Engineering and Core Store
2a Nivensknowe Road
Loanhead EH20 9AU
United Kingdom
iph@bgs.ac.uk

Scott Renshaw
Core Technician
British Geological Survey
Kingsley Dunham Centre
Keyworth
Nottingham HG12 5GG
United Kingdom

sren@bgs.ac.uk

Dave Smith†
Electronics Engineer
British Geological Survey
Marine Operations
Engineering and Core Store
2a Nivensknowe Road
Loanhead EH20 9AU
United Kingdom
dbsm@bgs.ac.uk

Hans-Joachim Wallrabe-Adams†
Database Operator
Institute for Marine Environmental Sciences
WDC-MARE/PANGAEA
University of Bremen
Leobener Strasse
D-28359 Bremen
Germany
hwallrabe@pangaea.de

Rolf Warthmann†
ESO Microbiologist
Department of Earth Sciences
Swiss Federal Institute of Technology
Geological Institute
Sonneggstrasse 5
8092 Zürich
Switzerland
warthmann@erdw.ethz.ch

Christian Wilson†
Staff Scientist in Training
British Geological Survey
Murchison House
West Mains Road
Edinburgh EH9 3LA
United Kingdom
ckw@bgs.ac.uk

Alex Wülbers†
Core Curator†**/Curatorial Specialist**
Bremen Core Repository (BCR)
Institute for Marine Environmental Research (MARUM)
Universität Bremen
Leobener Strasse
28359 Bremen
Germany
b11o@uni-bremen.de

SeaCore Personnel

Gary Jago
Offshore Manager

Stewart Frazer
Drill Superintendent

Andy Nesbit
Drill Superintendent

Martin Barnett
Electrician

Danny Bennetts
Drill Supervisor

Mike Court
Lead Driller

Terry Evans
Fitter

Rob Grenfell
Welder

Allan Pope
Drill Supervisor

Lee Pope
Driller

Simon Trewin
Drill Supervisor

University of Bremen Laboratory Staff

Vera Lukies
ESO Petrophysics Technician

Jens Grützner
ESO Petrophysics Support

Volker Diekamp
Photographer

Silvana Hessler
Chemistry Laboratory Technician

Karsten Enneking
Chemistry Laboratory Technician

Stefan Feil
Core Laboratory Technician (student)

Christian Mayer
Core Laboratory Technician (student)

Christiane Frenz
Core Laboratory Technician (student)

Hiederose Müller
Core Laboratory Technician (student)

Nike Fuchs
Core Laboratory Technician (student)

Susanne Schüller
Core Laboratory Technician (student)

Lena Röder
Core Laboratory Technician (student)

Susanne Schüller
Core Laboratory Technician (student)

Carola Schulz
Core Laboratory Technician (student)

Isabelle Schulz
Core Laboratory Technician (student)

Andrea Schwandt
Core Laboratory Technician (student)

Julia Wosniok
Core Laboratory Technician (student)

ABSTRACT

Integrated Ocean Drilling Program (IODP) Expedition 310 to the reef terraces around Tahiti, French Polynesia, was the second expedition to utilize a mission-specific platform (MSP) and was conducted by the European Consortium for Ocean Research Drilling (ECORD) Science Operator (ESO). The objectives of Expedition 310 are to establish the course of postglacial sea level rise at Tahiti, to define sea-surface temperature (SST) variations for the region over the period 20–10 ka, and to analyze the impact of sea level changes on reef growth and geometry. To meet these objectives, the postglacial reef sequence, which consists of successive reef terraces seaward of the living barrier reef, was cored from a dynamically positioned vessel during October and November 2005. A total of 37 boreholes across 22 sites were cored in water depths ranging from 41.65 to 117.54 m. Borehole logging operations in 10 boreholes provided continuous geophysical information about the drilled strata. The cores were described during the Onshore Science Party at the IODP Bremen Core Repository during February and March 2006, where minimum and some standard measurements were made. Further postcruise research on samples taken during the Onshore Science Party are expected to fulfill the objectives of the expedition.

INTRODUCTION

The timing and course of the last deglaciation is generally considered to be an essential component for understanding the dynamics of large ice sheets (Lindstrom and MacAyeal, 1993) and their effects on Earth's isostasy (Lambeck, 1993; Peltier, 1994). Moreover, the disappearance of glacial ice sheets was responsible for dramatic changes in the freshwater fluxes to the oceans, which disturbed the general thermohaline circulation and, hence, global climate (e.g., Stocker and Wright, 1991). Coral reefs, like the one that surrounds Tahiti, are excellent sea level indicators, and their accurate dating by mass spectrometry is of prime importance for determining the timing of deglaciation events and thus for understanding of the mechanisms driving glacial–interglacial cycles. Furthermore, scleractinian coral colonies can monitor and record past sea-surface temperatures (SSTs).

BACKGROUND

Sea Level Changes as a Global Climate Indicator

Only three deglaciation curves based on coral reef records have been accurately dated for times reaching the Pleistocene/Holocene boundary: in Barbados between 19.00 and 8.00 ka (Fairbanks, 1989; Bard et al., 1990a, 1990b), in New Guinea between 13.00 and 6.00 ka (Chappell and Polach, 1991; Edwards et al., 1993), and in Tahiti between 13.75 ka and 2380 ^{14}C y before present (BP) (Bard et al., 1996) (Fig **F1**). So far, the Barbados curve is the only one to encompass the whole deglaciation because it is based on offshore drilling. However, this site, like New Guinea, is located in an active subduction zone where tectonic movements can be large and discontinuous so that the apparent sea level records may be biased by variations in the rates of tectonic uplift. Hence, there is a clear need to study past sea level changes in tectonically stable regions or in areas where the vertical movements are slow and/or regular.

The Barbados record suggested that the last deglaciation was characterized by two brief periods of accelerated melting superimposed on a smooth and continuous rise of sea level with no reversals (Fig **F1**). These so-called meltwater pulse (MWP) events (MWP-1A and MWP-1B at ~13.80 and 11.30 ka, respectively) are thought to correspond to massive inputs of continental ice (i.e., ~50–40 mm/y, roughly equivalent to annual discharge rates of 16,000 km^3 for MWP-1A). MWP-1A corresponds to a short and intense cooling period between 14.10 and 13.90 ka in Greenland records (Johnsen et al., 1992; Grootes et al., 1993) and therefore postdates initiation of the

Bölling-Alleröd warm period at ~14.90–14.70 ka (Broecker, 1992). The sea level jump evidenced in New Guinea at 11.00 ka (Edwards et al., 1993) is delayed by a few centuries when compared to that observed at Barbados. These two meltwater pulses are thought to have induced reef-drowning events (Blanchon and Shaw, 1995). Two "give-up" reef levels have been reported at 90–100 and 55–65 m water depth on the Mayotte foreslopes (Comoro Islands) and have been related to the Bölling and the post-Younger Dryas meltwater pulses (Dullo et al., 1998); similar features are recorded in the southern Great Barrier Reef (GBR) (Troedson and Davies, 2001) and in the Caribbean (MacIntyre et al., 1991; Grammer and Ginsburg, 1992). A third Acropora reef-drowning event at ~7.60 ka has been assumed by Blanchon and Shaw (1995).

However, there are still some doubts concerning the general pattern of sea level rise during the last deglaciation events, including the amplitude of the maximum lowstand during the Last Glacial Maximum (LGM) and the occurrence of increased glacial meltwater with resultant accelerated sea level rise (Broecker, 1990). Furthermore, sawtooth sea level fluctuations between 19.00 and 15.28 ka (Locker et al., 1996) and a sea level fall coeval with climatic changes at ~11 ka are still controversial topics.

Worldwide sea level compilations indicate that local sea level histories varied considerably around the world in relation to both postglacial redistribution of water masses and a combination of local processes (Lambeck, 1993; Peltier, 1994), although significant deviations between model predictions and field data have been noted in several regions (Camoin et al., 1997). The post–last glacial sea level changes at sites located far away from glaciated regions ("far field") provide basic information regarding the melting history of continental ice sheets and the rheological structure of Earth. The effect of hydroisostasy depends on the size of the islands: for very small islands, the addition of meltwater produces a small differential response between the island and the seafloor, whereas the meltwater load produces significant differential vertical movement between larger islands or continental margins and the seafloor (Lambeck, 1993). There is therefore a need to establish the validity of such effects at two ideal sites located at a considerable distance from the major former ice sheets: (1) on a small oceanic island and (2) on a continental margin. In both cases, it is essential for the sites chosen that the tectonic signal is small or regular within the short time period proposed for investigation so that rigorous tests of proposed northern and southern hemisphere deglaciation curves from Barbados and New Guinea can be made. Two such places were proposed: Tahiti and GBR. This expedition conducted investigations at the Tahiti sites only.

Climatic and Oceanographic Changes during Last Deglaciation Events

During latest Pleistocene and early Holocene, climatic variability was primarily related to the effects of seasonality and solar radiation. The results of the Long-Range Investigation, Mapping, and Prediction (CLIMAP) program suggested that LGM tropical SSTs were similar to modern ones. However, this interpretation is not consistent with snowline reconstructions and paleobotanic data (Rind and Peteet, 1985; Anderson and Web, 1994).

The available Sr/Ca and U/Ca data from coral reef areas report SSTs 5˚C colder than those of today during the LGM and 2˚C lower at ~10–9 ka at Barbados (Guilderson et al., 1994), whereas studies in the west Pacific indicate that the full amplitude of the glacial Holocene temperature change may have ranged between 3˚ and 6˚C (McCulloch et al., 1996; Beck et al., 1997; Gagan et al., 1998) (Fig **F1**). Troedson and Davies (2001) define SSTs immediately south of the GBR some 4.5˚C colder during the LGM and 1˚C colder at 10 ka. This casts doubt upon the phase shift of 3000 y for climate changes between the two hemispheres that was assumed by Beck et al. (1997), in clear distinction to the apparent synchronism of the last deglaciation, inferred from various sources (i.e., coral records, ice cores, snowline reconstructions, vegetation records, and alkenone palaeothermometry) (Bard et al., 1997).

Recent studies have documented Holocene climatic variations. SSTs warmer by 1˚C, monsoonal rainfall, and possibly weaker El Niño–Southern Oscillation (ENSO) at ~5.80 ka in eastern Australia have been deduced from isotopic and Sr/Ca high-resolution measurements on corals from the central GBR (Gagan et al., 1998). An ENSO-like cyclic climatic variation with a return period of 3–5 y has been evidenced in a 4150 y old coral from the Seychelles, although the intensity of the annual decrease in SST caused by monsoonal cooling was lower than that of today (Zinke et al., 2005).

Additional information is required for better knowledge of climatic conditions in tropical regions during the last deglaciation. In these areas, the most debated points are twofold: (1) the quantification of SSTs and the identification of related climatic variations during the last deglaciation events and (2) the timing of the relevant postglacial warming in the two hemispheres.

SCIENTIFIC OBJECTIVES

1. Establish the course of postglacial sea level rise at Tahiti (i.e., define the exact shape of the deglaciation curve for the period 20.00—10.00 ka.

In establishing the deglaciation curve, we hope to assess the validity, timing, and amplitude of the MWP-1A event, assess the maximum sea level drop during the LGM to prove or disprove the sawtooth pattern of sea level rise during the last deglaciation (Locker et al., 1996), and test predictions based on different ice and rheological models.

Reconstruction of sea level curves relies on absolute dating of in situ corals by radiometric methods ($^{230}Th/^{234}U$ by thermal ionization mass spectrometry [TIMS] and ^{14}C by accelerator mass spectrometry [AMS]) and paleobathymetric information deduced from biological communities (corals, algae, and mollusks) that live in a sufficiently narrow or specific depth range to be useful as absolute sea level indicators.

2. Define SST variations for the region over the period 20.00—10.00 ka

This information is needed to gain better knowledge of regional variation of SSTs in the South Pacific, climatic variability and identification of specific phenomena such as ENSO, and global variation and relative timing of postglacial climate change in the southern and northern hemispheres.

Methods include stable isotope ($\delta^{18}O$) and trace element (Sr/Ca ratios by TIMS) analyses on high-resolution (i.e., at the monthly scale) sampling of massive coral colonies. Coupled analyses of $\delta^{18}O$ and Sr/Ca on the same sample may yield estimates of both temperature and salinity (McCulloch et al., 1996). Stable isotope $\delta^{18}O$ measurements, systematically coupled with those of $\delta^{18}O$ in coral skeletons, will provide information on other parameters (e.g., solar variations or metabolism processes). Geochemical methods will be coupled with measurements and analyses of the bandwidths and microstructural variations in the coral skeletons.

3. Analyze the impact of sea level changes on reef growth and geometry.

Assessments will be made of the impact of glacial meltwater phases (identification of reef drowning events) and the morphological and sedimentological evolution of the foreslopes (highstand versus lowstand processes). In addition, modeling of reef building and analyses of environmental changes during reef development will be undertaken.

A numerical model simulating reef building will be used to study the effect of a sea level jump on reef geometry and to qualitatively assess the effect of sea level fluctuations on the reef shape and age-depth relationships.

Expedition 310 may provide the opportunity to better constrain deglacial history (see Peltier, 1994; Fleming et al., 1998; Okuno and Nakada, 1999) by documenting, for the first time, the LGM lowstand in well-studied cores in the far field and by comparing the MWP-1A event in the Pacific and Atlantic Oceans. Furthermore, study of very early deglacial coral material should provide the first Sr/Ca SSTs for the LGM in the Pacific, which could then supplement Barbados sample data (Guilderson et al., 1994) and the recent study of Stage 6 corals (McCulloch et al., 1999).

OPERATIONAL STRATEGY

Drilling offshore Barbados (Fairbanks, 1989) demonstrated that the reef sequence corresponding to the last deglaciation developed only on slopes and therefore forms discontinuous successive terraces of various lateral extent.

At Tahiti, recovery of the postglacial reef sequence required drilling successive reef terraces that occur seaward of the living barrier reef. Studies and surveys around Tahiti have demonstrated the occurrence of successive reef terraces at various depths, 100, 90, 60, and 40–50 m, which therefore correspond to drilling targets. Thus, at each site, we cored several boreholes along transects to attempt to recover the entire postglacial reef sequence.

Based on the results of previous scientific drilling and bathymetric and seismic data acquired during the SISMITA cruise, we drilled a transect of holes in three areas around Tahiti: offshore Papeete-Faaa (proposed Site TAH-01A), Tiarei (proposed Site TAH-02A), and Maraa (proposed Site TAH-03A) (Fig. **F2**). The involved water depths ranged from 41.65 to 117.54 m.

The exact location of the drill holes was determined during the cruise by checking the nature and morphology of the seafloor with a through-pipe underwater camera. All holes were sited within a circle of radius 150 m around the proposed drilling sites approved by the Environmental Pollution and Safety Panel (EPSP), or within the mid-cruise EPSP-approved 200 m extension of the circle around proposed Site TAH-02A-4 (to 350 m radius). Figures **F3, F4,** and **F5** show the locations of the holes at Faaa, Tiarei, and Maraa, respectively.

SITE RESULTS

Cores were recovered from 37 holes across 22 sites (M0005 to M0026) (Table **T1**), with a conventionally calculated recovery of 57.47%. Water depths at the sites ranged from 41.6 to 117.5 m, and cores were recovered from 41.6 to 161.8 meters below sea level (mbsl). Because of difficulties locating and operating at some the proposed drill sites (see **Operations**), the original strategy of coring along profiles was abandoned and new sites were chosen on the basis of water depth. Thus six drilling "areas" were targeted: Faaa, Tiarei inner ridge, Tiarei outer ridge, Tiarei marginal sites, Maraa western transect, and Maraa eastern transect. All new sites were drilled within areas approved by EPSP. Borehole geophysical wireline logging was conducted at seven sites (in ten holes).

Because of space limitations on the *DP Hunter,* only limited analysis of cores was conducted offshore, with the bulk of description and measurement conducted at the Onshore Science Party at the Bremen Core Repository. Table **T2** shows which measurements were conducted offshore and at the Onshore Science Party.

Sedimentology and Biological Assemblages

The cored material shows that the reefs around Tahiti are composed of two major lithological units: a postglacial carbonate sequence (Unit I) and an older Pleistocene sequence (Unit II). Modern sediments were often recovered above Unit I. Within Units I and II, the lithostratigraphy can be divided into subunits (e.g., Subunit IA, IB, IC, and so on), based on coral assemblages and internal structure. It is important to note that subunits of the same designation at separate sites are not correlative. Correlation of subunits between sites will not be possible until ages are obtained from postcruise research.

Maraa Western Transect: Sites M0005, M0006, and M0007

The western transect drilled in the Maraa area (southwest Tahiti) includes Sites M0007, M0005, and M0006 (landward to oceanward) in water depths between 43 and 82 m. Figure **F6** summarizes the major lithologic units, lithology, and recovery for all holes on the Maraa western transect.

Modern Sediments

Modern sediments were recovered at all sites along this transect. They consist of a few decimeter-thick beds comprising rhodoliths, skeletal sands, and gravels rich in *Halimeda* segments, mollusk fragments, benthic foraminifers, and nongeniculate coralline algae along with clasts of *Halimeda* packstone and coral clasts.

Lithologic Unit I (Postglacial Carbonate Sequence)

The thickness of Unit I ranges from 33 to 42 m at Sites M0005 and M0007, respectively.

The top of Unit I is characterized by an abundance of thin crusts of nongeniculate coralline algae and extensive bioerosion. This sequence is primarily composed of coralgal-microbialite frameworks commonly interlayered with loose skeletal sediments including coral and algal rubble and skeletal sand and with skeletal limestone.

The coralgal-microbialite frameworks that form the bulk of this unit are characterized by widespread development of microbialites which locally represent the major structural and volumetric component of the reef rock. They develop within the primary cavities of the reef framework, where they generally overlie crusts of noneniculate coralline algae. The microbialites generally comprise a suite of fabrics including two end-members represented by laminated fabrics and thrombolitic accretions; the laminated fabrics generally correspond to the most abundant fabric.

The reef sequence is characterized by a general succession of distinctive coral assemblages, although many of them are intergradational, both laterally and vertically. Two successive subunits (Subunits IA and IB) displaying distinctive coral assemblages and internal structure were recognized:

- Subunit IA, up to 20 m thick, primarily comprises coralgal-microbialite frameworks dominated by encrusting coral colonies.
- Subunit IB, up to 25 m thick, comprises coralgal-microbialite frameworks made of tabular and branching coral colonies that are usually heavily encrusted by noneniculate coralline algae, locally associated with vermetid gastropods, overlain by very thick and massive microbialite crusts. Large primary cavities are partially filled with skeletal sand rich in *Halimeda* segments and coral fragments.

At Site M0007, the base of Subunit IB corresponds to poorly lithified skeletal grainstone that contains fine sand-sized volcanic grains and a 30 cm thick interval composed of branching coralline algae in Core 310-M0007B-34R.

Lithologic Unit II (Older Pleistocene Sequence)

The top of Unit II was recovered at 86 and 92 mbsl at Sites M0005 and M0007, respectively. This sequence was drilled to 161.56 mbsl in Hole M0005D.

The older Pleistocene sequence is composed of eight distinctive lithologic subunits:

- Subunit IIA is a beige to gray well-lithified limestone comprising coralgal frameworks associated with rudstone-floatstone beds.
- Subunit IIB is a well-lithified skeletal floatstone-rudstone rich in rhodoliths, fragments of corals and mollusks, and *Halimeda* segments, associated with volcanic grains.
- Subunit IIC is a poorly sorted and ungraded unlithified volcaniclastic silt to sand including scattered skeletal grains reworked pebbles of *Halimeda* floatstone and angular clasts of siltstones of the same composition.
- Subunit IID is a beige to brownish coralgal framework in which corals are thinly coated by nongeniculate coralline algae and then heavily encrusted by microbialites with laminar and thromboltic fabrics.
- Subunit IIE is a sandy skeletal grainstone rich in volcanic grains, large coral clasts (massive *Porites*), and skeletal fragments (coralline algae and corals).
- Subunit IIF is a coral and algal rudstone to floatstone comprising fragments of corals (massive, encrusting, and branching corals), coralline algae, echinoids and mollusks, rhodoliths, and lithoclasts in a coarse sandstone matrix rich in volcanic and skeletal grains.
- Subunit IIG is a coralgal framework interbedded with skeletal grainstone to packstone rich in volcanic grains.
- Subunit IIH is a skeletal grainstone to floatstone rich in fragments of corals (branching *Pavona* and encrusting *Montipora*), echinoids and coralline algae, and volcanic grains.

Maraa Eastern Transect: Sites M0015, M0016, M0017, and M0018

The eastern transect drilled in the region of Maraa (southwest Tahiti) includes Sites M0017, M0015, M0018, and M0016 (landward to oceanward) in water depths from

56.45 to 97.35 mbsl. Figure **F7** summarizes the major lithologic units, lithology, and recovery for all holes on the Maraa eastern transect.

Lithologic Unit I (Postglacial Sequence)

The thickness of Unit I ranges from 24 m in the deepest hole (Hole M0016B at 97.35 mbsl) to 40 m in Hole M0018A. The base the unit has been recovered from 94 mbsl at the inner sites to 121 mbsl at the outer sites.

This unit is primarily composed of coralgal-microbialite frameworks commonly interlayered with loose skeletal sediments including coral and algal rubble. Coral and algal rubble are mostly composed of accumulations of fragments of corals (mostly encrusting *Acropora* and *Montipora* and branching *Pocillopora* and *Porites*), microbialites and mollusks, *Halimeda* segments, and rounded lithoclasts (e.g., skeletal sandstone rich in volcanic grains). Benthic foraminifers are usually scarce. Pebbles of basalt and sand-sized volcanic grains occur locally. Skeletal sand corresponds to *Halimeda* sand rich in fragments of corals (e.g., branching *Porites*) echinoids and mollusks.

The frameworks that form the bulk of Unit I include three subunits (Subunits IA–IC) displaying distinctive coral assemblages and internal structure. Corals are usually thinly encrusted by nongeniculate coralline algae, except in Subunit IC, where the crusts are significantly thicker (up to 2 cm thick) and include vermetid gastropods. The last stage of encrustation over coral colonies corresponds to thick microbialite crusts dominated by massive laminated fabrics.

- Subunit IA primarily comprises locally well lithified coralgal bindstone that forms the upper part of Unit I in all holes. In Holes M0015B and M0018A, the top of the subunit is characterized by the occurrence of a hardground and a yellow-reddish staining of the rock surface. The coral assemblages are dominated by encrusting (*Montipora, Pavona*, *Porites, Leptoseris,* and *Leptastrea*) and foliaceous coral colonies (*Pachyseris*). Associated corals include massive *Porites* and branching colonies of *Porites*, *Pavona,* and *Pocillopora* (including robust branching colonies). Tabular colonies of *Acropora* occur in the lower part of the subunit.
- Subunit IB is mostly composed of coralgal-microbialite frameworks in which the coral assemblages are dominated by tabular colonies of *Acropora*. Associated corals include encrusting colonies of *Montipora* (locally dominant), *Porites*, *Leptastrea*, *Montastrea,* and agaricids, massive colonies of *Porites* and *Montastrea*, branching colonies of *Porites*, *Pocillopora,* and *Acropora*. Robust branching colonies of *Acropora*

and *Pocillopora* occur in the lower part of the subunit, where they are locally dominant.

- Subunit IC comprises coralgal-microbialite frameworks dominated by branching colonies of *Porites*. The coral assemblage associated with the branching colonies of *Porites* is well diversified and includes branching colonies of *Pocillopora* and *Acropora*, robust branching colonies that are locally dominant, encrusting colonies of *Porites, Montipora*, *Leptastrea*, *Millepora*, *Pavona*, *Leptoseris,* and *Psammocora,* and tabular colonies of *Acropora*.

Lithologic Unit II (Older Pleistocene Sequence)

Unit II is primarily composed of irregular alternations of yellow and gray to beige poorly sorted skeletal limestone (grainstone to rudstone-floatstone) and coralgal frameworks with local intercalations of coral and algal rubble that display conspicuous alteration.

Subaerial diagenetic processes are indicated by recrystallization of coral skeletons and the occurrence of large solution cavities that display yellow and brown to red-brown staining. Some solution cavities are partly filled with sediments.

The grainstones, rudstones, and floatstones are rich in fragments of corals (e.g., robust branching *Pocillopora*, branching and massive *Porites*, branching *Acropora,* and encrusting *Montipora*), coralline algae, echinoids and mollusks, and *Halimeda* segments. Sand-sized volcanic grains are commonly associated with the skeletal grains.

The coralgal frameworks comprise encrusting and branching colonies of *Porites*, tabular colonies of *Acropora*, encrusting and massive colonies of *Montipora*, and encrusting colonies of agaricids; massive colonies of *Porites* occur locally.

Tiarei Inner Ridge: Site M0023

Figure **F8** summarizes the major lithologic units, lithology, and recovery for all holes on the Tiarei inner ridge.

Lithologic Unit I (Postglacial Sequence)

Unit I is primarily composed of coralgal-microbialite frameworks. Manganese(?) impregnation and dark staining of corals is reported at the top of the unit. Basalt pebbles and volcanic grains are abundant toward the base of the unit.

Unit I is characterized by three successive coral assemblages (Subunits IA–IC):

- Subunit IA consists of encrusting colonies of *Montipora*, *Pavona*, *Porites,* and acroporids, foliaceous colonies of *Pachyseris* associated with branching colonies of *Porites,* and, to a less extent, robust branching colonies of *Pocillopora.*
- Subunit IB consists of massive and encrusting colonies of *Porites* and faviids (*Leptastrea*) and, to a less extent, branching colonies of *Porites* that occur locally.
- Subunit IC consists of branching and encrusting colonies of *Porites* associated with encrusting colonies of *Millepora*, *Montipora, Psammocora,* and *Pavona*, massive colonies of *Leptastrea* and *Porites*, branching colonies of *Pocillopora* (including robust branching colonies), and tabular colonies of *Acropora* (*A. humilis*?).

Lithologic Unit II (Older Pleistocene Sequence)

Unit II comprises brown algal bindstone, microbialites, and coralgal frameworks that exhibit evidence of diagenetic alteration including the neomorphic transformation of coral skeletons and the occurrence of solution cavities. Basalt pebbles and lithoclasts occur throughout this unit.

Solution cavities present throughout this interval are filled with multigenerational infillings including well-lithified pale brownish limestone and poorly lithified dark brown sandy sediments including skeletal grains.

The coral assemblage includes massive and encrusting colonies of faviids, robust branching and tabular colonies of *Acropora*, encrusting colonies of agaricids, and branching colonies of *Porites*.

Tiarei Outer Ridge: Sites M0009, M0021, M0024, M0025, and M0026

Figure **F9** summarizes the major lithologic units, lithology, and recovery for all holes on the Tiarei outer ridge.

Lithologic Unit I (Postglacial Sequence)

On the outer ridge of Tiarei, Unit I was recovered from 82 to 122 mbsl. The thickest continuous sequence was recovered from Holes M0021A and M0021B, in which its thickness reaches 29 m.

Unit I mostly comprises coralgal-microbialite frameworks that are locally interlayered with volcaniclastic sediments including coarse sand displaying skeletal elements (foraminifers, *Halimeda* segments, fragments of mollusks, bryozoans, corals, and espe-

cially branching *Porites*), rubble and sand composed mostly of coral fragments (mostly branching colonies and, to a lesser extent, tabular colonies), and skeletal packstone to floatstone rich in *Halimeda* segments and coral and mollusk fragments.

The top of Unit I is characterized by widespread development of micritic microbial crusts that display laminar and knobby morphologies. Extensive bioerosion, dark to brown staining within the uppermost 2–3 m of the unit, and hardgrounds are features that have been locally observed.

Coralgal-microbialite frameworks are characterized by distinctive internal structure and coral assemblages. Five lithologic and coral assemblages (Subunits IA–IE) display a general consistent trend:

- Subunit IA, the uppermost assemblage, is dominated by encrusting colonies of *Montipora, Montastrea, Leptastrea, Pavona,* and *Porites* and encrusting foliaceous colonies of *Pachyseris* and *Leptoseris*.
- Subunit IIA is dominated by branching and encrusting colonies of *Porites* and *Montipora*; associated corals include encrusting and branching colonies of *Pavona* and, to a lesser extent, branching colonies of *Pocillopora*, tabular colonies of *Acropora,* and encrusting colonies of agaricids.
- Subunit IC is dominated by massive colonies of *Porites*; some colonies display traces of bioerosion.
- Subunit ID is dominated by colonies of robust branching *Pocillopora* and encrusting colonies of favids and encrusting and branching colonies of *Montipora*.
- Subunit IE, the bottommost assemblage, is composed of encrusting and massive colonies of favids (*Favia* and *Leptastrea*) locally associated with encrusting colonies of *Montipora*. Associated coral rubble comprises mostly fragments of branching *Porites*, *Acropora,* and *Pocillopora*.

The development and morphologies of the microbial crusts are closely related to the morphology and size of the cavities in which they developed. In bindstone formed by encrusting coral assemblages, the microbialites are dominated by thrombolitic fabrics, whereas in frameworks made of branching and massive coral colonies they display greater development and are characterized by the development of compound crusts, up to 15 cm thick, formed by a succession of laminated and thrombolitic fabrics, where the thrombolites usually represent the last stage of encrustation. The thrombolites consist of closely spaced and vertically and laterally intergradational micritic masses that range from narrow millimeter-sized upward-radiating shrubs to

broader dendritic clusters as high as 1 cm. Multiple generations may be closely packed and merge into micritic crusts as thick as several centimeters.

Lithologic Unit II (Older Pleistocene Sequence)

The contact between Units I and II is characterized by an irregular unconformity typified by an abundance of large solution cavities partly filled with unconsolidated skeletal and volcanic sand including coralline algal branches and *Halimeda* segments and coral gravels (*Pocillopora* branches and fragments of *Montipora* colonies). Some cavities are partly filled with skeletal and volcanic sands and gravels and stalagmite crusts. Several unconformities occur in the upper part of Unit II.

Unit II comprises four lithologic subunits (Subunits IIA–IID) that are locally interlayered:

- Subunit IIA is composed of well-lithified gray to brown coralgal frameworks with coral assemblages dominated by encrusting colonies of *Leptastrea, Pachyseris, Montipora,* and *Psammocora*, locally associated with robust branching colonies of *Acropora* and *Pocillopora*, tabular colonies of *Acropora*, and massive colonies of *Porites* associated with coral rudstone-floatstone and skeletal limestone.
- Subunit IIB comprises coral clasts, limestone clasts, basalt pebbles, and reworked coral colonies (*Porites* and robust branching *Acropora*).
- Subunit IIC is a sandy packstone/grainstone with coral clasts (branching *Acropora* and *Pocillopora*) overlying a coral boundstone consisting mainly of massive *Porites* and encrusting unidentified corals associated with clasts of robust branching *Acropora*.
- Subunit IID is a massive weakly consolidated and cemented dark gray to brownish volcaniclastic siltstone to sandstone that includes pieces of corals (branching *Pocillopora* and encrusting *Montipora*) and coralline algal crusts and skeletal fragments (tiny mollusk shells and *Halimeda* segments) interlayered with sandy limestone and granule- to pebble-sized pieces of aphanitic dense basalt.

Tiarei Marginal Sites: Sites M0008, M0010, M0011, M0012, M0013, M0014, and M0022

Sequences Dominated by Volcaniclastic Sediments

Hole M0008A exhibits a 36 m thick sequence (64.15–100.05 mbsl) composed of two lithological units:

- Unit I is a black uncemented to weakly consolidated volcaniclastic sand, silt, and clay interlayered with beds comprising basalt pebbles, cobbles, and boulders.

- Unit II is a orange, dark brown, to reddish brown volcaniclastic siltstone to sandstone interlayered with volcaniclastic sand and silt, volcaniclastic cobble, and rubble.

The boundary between the two units is marked by a change from silts/sands to siltstone/sandstone and a color change from gray to orange-brown. Coincidentally, in Hole M0021B, a similar color change coincides with the Unit II/I boundary. Figure **F10** summarizes the major lithologic units, lithology, and recovery for all holes of the Tiarei marginal sites.

Lithologic Unit I (Postglacial Sequence)

In holes located close to the outer ridge (Holes M0010A through M0014A), Unit I comprises three successive subunits (Subunits IA–IC) that were recovered from 78.85 to 117 mbsl:

- Subunit IA was recovered only at Site M0012 from 78.85 to 107 mbsl. It is mostly composed of loose sediments (coral rubbles and skeletal silt and sand) locally interlayered with volcaniclastic sand rich in skeletal grains.
- Subunit IB, recovered in an interval ranging generally from 90 to 100–105 mbsl, is dominated by volcaniclastic sediments that are locally interlayered with beds comprising carbonate elements and coral colonies.
- Subunit IC, ranging generally from 100 to 115 mbsl, is primarily comprised of coralgal-microbialite frameworks interlayered with beds composed of (1) coral rubble, fragments of coralline algal crusts, and microbialites mixed with sand- to pebble-sized volcanic elements; (2) skeletal sand rich in *Halimeda* segments, foraminifers, and fragments of mollusks and coralline algae mixed with volcanic grains; and (3) volcaniclastic and skeletal sand and silt. The frameworks comprise two distinctive coral assemblages:
  1. The first assemblage is dominated by encrusting *Montipora,* agaricids, and faviids and thin branching colonies of *Porites*.
  2. The second assemblage consists of massive colonies of *Porites* and faviids locally associated with branching *Pocillopora* and *Montipora*.

Lithologic Unit II (Older Pleistocene Sequence)

The boundary between Units I and II is sharp. Unit II is composed mainly of well-lithified gray to light brown coralgal boundstone, coral rudstone, and skeletal sandy limestone, interlayered locally with horizons of gravels and rubble made of that ma-

terial. The coral assemblage is dominated by foliaceous colonies of *Pachyseris*, tabular and branching colonies of *Acropora*, robust branching *Pocillopora*, encrusting and branching colonies of *Montipora,* and branching and massive colonies of *Porites*. Microbialites are abundant and include laminated and thrombolithic fabrics. The matrix of the limestone is rich in *Halimed*a segments; volcanic grains are locally abundant. Subaerial diagenetic processes are indicated by the alteration of coral skeletons and the occurrence of large solution cavities that are filled with volcaniclastic and skeletal sandstone and by gravels and rubble including branches of *Pocillopora* and basalt pebbles at the top of the unit.

Faaa: Sites M0019 and M0020

The following description concerns Sites M0019 and M0020, which were drilled at 59.9 and 83.7 mbsl, respectively. The location of the boundary between Units I and II in the two holes was defined on the basis of lithologic and diagenetic features; it occurs at 82 m in Hole M0019A and at 92 m in Hole M0020A. Figure **F11** summarizes the major lithologic units, lithology, and recovery for all holes of the Faaa sites.

Lithologic Unit I (Postglacial Sequence)

Unit I at Sites M0019 and M0020 is 21 and 8 m thick, respectively, and displays a very similar composition in the two holes. It primarily comprises loose coralgal-microbialite frameworks (bindstone) interlayered with beds of coral rubble. The beds of coral rubble are composed of reworked and rounded fragments of corals (branching agaricids and *Porites*), coralline algal crusts, and microbialites that are extensively bored and stained.

The coralgal-microbialite frameworks are dominated by encrusting colonies of *Montipora*, agaricids (*Pavona*?), *Acropora, Psammopora,* and *Echinophyllia* associated locally with massive colonies of *Porites*, *Montastrea*, *Cyphastrea,* and *Leptastrea* and encrusting colonies of *Leptoseris* and fragments of robust branching colonies of *Pocillopora*, tabular colonies of *Acropora,* and branching *Porites* in addition to the coral colonies listed before. Microbialites consist of dark gray laminated dense and thrombolitic fabrics; the latter are usually dominant. Large cavities, partly to fully filled with skeletal sand rich in *Halimeda* segments (*Halimeda* packstone), commonly occur. Reddish brown to dark staining on the surface of reef rocks is conspicuous in some cores.

Lithologic Unit II (Older Pleistocene Sequence)

Unit II at Sites M0019 and M0020 is 43 and 33 m thick, respectively, and displays a distinctive composition in the two holes. The coralgal-microbialite frameworks in the bulk of this unit are characterized by the widespread development of microbialites.

In Hole M0019A, Unit II includes three subunits (Subunits IIA–IIC), characterized by their distinctive lithology and composition and separated by unconformities at 106.2 and 121.12 mbsl, respectively:

- Subunit IIA is 24 m thick and comprises irregular alternations of beige coralgal and skeletal limestone bearing in situ coral colonies and beds of coral rubble. The coral assemblages forming the coralgal frameworks consist of massive colonies of *Porites*, branching and encrusting colonies of *Porites,* and, to a lesser extent, encrusting colonies of agaricids*, Montipora* and *Millepora*, massive colonies of *Leptastrea* and *Montastrea*, and tabular colonies of *Acropora*. Fragments of branching colonies of *Pocillopora* occasionally occur. The skeletal limestone consists of a well-lithified rudstone including subrounded coral fragments (branching and massive *Porites*, robust branching *Pocillopora*, and tabular *Acropora*) often encrusted by coralline algae and locally surrounded by cement fringes. Other skeletal grains include *Halimeda* segments and fragments of echinoids, coralline algae, and mollusks.
- Subunit IIB is 15 m thick and comprises yellowish brown skeletal floatstone to grainstone including rhodoliths, foraminifers, and fragments of corals (branching and encrusting *Porites*, robust branching *Pocillopora*, and tabular *Acropora*) and coralline algae, echinoids, and mollusks; sand-sized volcanic grains occur in the lower part of the subunit and their abundance increases downhole.
- Subunit IIC is 11 m thick and comprises irregular alternations of coralgal frameworks, skeletal limestone, and rubble beds. The coralgal frameworks are dominated by tabular colonies of *Acropora*, massive colonies of *Porites* (e.g., Cores 310-M0019A-27R and 28R), encrusting colonies of *Porites* and *Montipora*, and robust branching colonies of *Acropora*. The skeletal limestone consists of a very poorly sorted rudstone rich in large coral fragments (tabular *Acropora*, robust branching *Pocillopora*, branching *Porites*, and encrusting agaricids), rhodoliths, *Halimeda* segments and fragments of coralline algal crusts, mollusks, and echinoids.

In Hole M0020A, Unit II is primarily composed of coralgal frameworks locally interlayered with skeletal limestone and rubble beds. The coralgal frameworks are dominated by branching and encrusting *Porites*, locally associated with encrusting *Montipora* and *Pavona*, and robust branching colonies of *Pocillopora*. The interlayered

skeletal limestone consists of *Halimeda* wackestone and poorly sorted coral rudstone including fragments of branching and encrusting *Porites*, robust branching *Pocillopora* and *Acropora*, and encrusting *Montipora*. Other skeletal grains include *Halimeda* segments and fragments of mollusks and echinoids; volcanic silt to sand grains are locally abundant.

Physical Properties

Carbonates are major constituents of the sedimentary rock record. Because coralgal reefs develop in shallow water, they are interesting systems to study. These kinds of sedimentary systems are most sensitive to climate and sea level fluctuations but also have great aquifer and reservoir potential. From a rock physics point of view, Expedition 310 was particularly interesting because it provided the unique opportunity to (petro)physically quantify modern reef development before pronounced overprinting by diagenetic processes (including mechanical compaction), which usually results in irresolvable complexities as very often encountered in aquifer and reservoir characterization.

A crossplot of velocity versus porosity for all sites shows a negative inverse relationship (Fig. **F12**) between acoustic velocity (V_P) and porosity. Instead of showing individual data points for the bulky multisensor core logger (MSCL) data (15,191 data points), data density was contoured. MSCL data were acquired cross core (over ~6.5 cm), whereas core plugs were never longer than 3 cm and could only be drilled in appropriate core sections. The scale dependency of petrophysical measurements, along with the (inevitable) difference in "selective" sampling of core as opposed to bulk MSCL measurements is beautifully illustrated in Fig. **F12:** for a given porosity value, discrete measurements have higher V_P values than MSCL measurements. Furthermore, in the comparison of velocity modeled using widely used velocity models and the real data, the modified (to improve relationships observed in larger-scale investigation of downhole wireline logging data) Raymer time average equation (Raymer et al., 1980) gives the best fit (smallest error) with MSCL data, whereas the Wyllie equation (Wyllie et al., 1958) shows the best fit for discrete samples. However, the difference between both velocity transforms and the real data points is still high. On the high end of the range in velocity for a given porosity, these differences can be interpreted as the added effect of pore characteristics like pore shape and connectivity and textural properties of the (overall coralgal) framework. The differences on the low end of the range in velocity for a given porosity may very well originate from lack of burial compaction and/or pronounced diagenesis.

Downhole Logging

Downhole geophysical logs provide continuous information on physical, chemical, textural, and structural properties of geological formations penetrated by a borehole. In intervals of low or disturbed core recovery, downhole geophysical logs provide the only way to characterize the borehole section. This is especially true when recovery is poor and when comparable measurements or observations are obtained from core, as downhole geophysical logging allows precise depth positioning of core pieces by visual (borehole images) or petrophysical correlation.

Borehole Geophysical Instruments

The set of borehole geophysical instruments utilized during Expedition 310 was constrained by the scientific objectives and the geological setting of the expedition. A suite of downhole geophysical methods was chosen to obtain high-resolution images of the borehole wall, to characterize the fluid nature in the borehole, to measure borehole size, and to measure or derive petrophysical or geochemical properties of the formation such as porosity, electrical resistivity, acoustic velocities, and natural gamma radioactivity. Because of environmental constraints, no nuclear tools were deployed during Expedition 310.

The slimline suite comprised the following tools:

- Optical Borehole Televiewer (OBI 40) produces a millimeter-scale, high-resolution image of the borehole wall, similar to a subsurface endoscope.
- Acoustic Borehole Televiewer (ABI 40) produces millimeter-scale, high-resolution images of the borehole surface using acoustic pulse and echo techniques.
- Hydrogeological probe (IDRONAUT) measures hydrogeological properties of the borehole fluid only.
- Spectral Natural Gamma Probe (ASGR) allows identification of the individual elements that emit gamma rays (potassium, uranium, and thorium).
- Induction Resistivity Probe (DIL 45) provides measurements of electrical conductivity. The output of the tool comprises two logs: ILM (induction electrical conductivity of medium investigation depth, 0.57 m) and ILD (induction electrical conductivity of greater investigation depth, 0.83 m). The measured conductivity is finally converted into electrical resistivity.

- Full Waveform Sonic Probe (SONIC). The 2PSA-1000 sonic probe measures compressional wave velocities of the formation. In addition, analysis of surface waves in the borehole (i.e., Stoneley waves) can be indicative of formation permeability.
- Caliper Probe (CAL). The 2PCA-100 is a three-arm (mechanical) caliper tool that measures the borehole diameter.

A total of 10 boreholes were prepared for downhole geophysical measurements. All measurements were performed under open borehole conditions (no casing) with the exception of a few of spectral gamma ray logs. After completion of coring, the drill string was pulled and the coring bit was changed for an open shoe casing to provide borehole stability in unstable sections and a smooth exit and entry of logging tools. In addition, a wiper trip was performed with fresh seawater (no drilling mud was used). Borehole conditions were extremely hostile, and very often the boreholes had to be logged in intervals where the HQ drill string was used as temporary casing, resulting in a nominally 100 mm diameter borehole. In order to record ultra-high-resolution geophysical downhole logging data, the acquisition was done in the rooster box, which, in the used piggy-back drilling system, is heave-compensated. Because of these difficult borehole conditions and time constraints it was not possible to log all tools in every borehole.

Preliminary Results

Wireline logging operations at the Tiarei sites produced nearly complete downhole coverage of lithologic Unit I from 72 to 122 m below present-day sea level (Fig. **F13**). Because of very hostile borehole conditions around the Unit II/I boundary, it was not possible to image this boundary properly, with the exception of Hole M0023B.

The measured geophysical parameters, including optical and acoustic borehole wall images, provided the only source of continuous information of the drilled sequences during Expedition 310. Furthermore, by "unrolling" the images of the borehole wall (360°), into a two-dimensional view, a cross section ~31 cm is obtained as compared to a 6.54 cm cross section of a split core obtained by HQ-diameter drill bit. It was therefore possible to identify a typical stacking of lithofacies from the continuous downhole geophysical logs. A typical stacking of facies is grouped into a subsequence.

A subsequence consists of three lithofacies: a basal lithofacies, middle lithofacies, and an uppermost lithofacies:

- The basal lithofacies of a typical subsequence consists of fragments of branching coral colonies in a sandy/muddy matrix at proximal locations, has elevated values in natural radioactivity, low electrical resistivity values, and lowest acoustic velocities. At distal locations, this facies is characterized by extremely open coral framework or medium-sized cavities.
- The middle lithofacies of a subsequence consists of branching coral colonies (Fig. **F13**) in which framework density usually increases toward the top. It is characterized by upsection decreases in natural radioactivity and increases in electrical resistivity and acoustic velocities.
- The uppermost lithofacies of a typical subsequence consists of foliaceous to tabular and encrusting coral species and minor massive corals (*Porites*). It is characterized by intermediate to lower acoustic velocities, decreasing resistivity values upsection, and increasing natural radioactivity values.

In Figure **F13,** borehole images and natural radioactivity logs (total counts only) are plotted in meters below present-day sea level. In each of the logged boreholes, the boundary between lithologic Unit II and Unit I is indicated. In the Tiarei transect, the basal unit directly overlying the above-mentioned boundary consists of a semiconsolidated rubble interval having elevated natural gamma radioactivity values in proximal locations. Distal locations do not show this higher gamma ray signature and, although poorly recovered in downhole logging data, it usually consists of very open framework branching corals that are heavily encrusted.

In Figure **F14,** borehole images and formation electrical resistivity (resistivity) are plotted in meters below present-day sea level. At this larger scale of observation and by correlating the boreholes from the outer ridge to the inner ridge, it becomes clear that, although evolved on a relatively steep and irregular paleomorphology, the general resistivity pattern and absolute values of lithologic Unit I along this transect are essentially the same and comparable. In each borehole the basal interval has lowest resistivity values, values increase gradually to a maximum value, after which a more sharp negative excursion to lower values can be observed. The interval of increasing resistivity values is interrupted by a subtle but clear decrease in the middle of lithologic Unit I. The absolute values of this decrease are higher in distal boreholes than in the proximal boreholes.

Wireline logging operations at the Maraa sites produced nearly complete downhole coverage of lithologic Unit I from 102 to 41.65 m below present-day sea level (Fig. **F15**). Very hostile borehole conditions are caused by open framework coral morphol-

ogies and relatively soft microbialite encrusting along and over coral colonies. Overall, acoustic reflectivity values in the ABI-40 image logs are lower than those at Tiarei. These conditions did not allow image "recovery" as high as that for the Tiarei transect and, similar to Tiarei, the boundary between lithologic Units I and II could not be imaged. Spectral gamma ray logs through the steel casing do, however, indicate significant count increases in lithologic Unit II. In Figure **F15,** borehole images, natural radioactivity logs (total counts only), and electrical resistivity logs are plotted in meters below present-day sea level. In each of the logged boreholes, the boundary between lithologic Units I and II is indicated. The depth below present-day sea level of the Pleistocene boundary depends on paleoseafloor morphology at the time of the LGM. Although the quality and meters covered in imaging lithologic Unit I is less at Maraa than at Tiarei, a similar stacking of lithofacies can be identified.

Microbiology

Drill core samples from Tahiti reefal environments were analyzed for evidence of microbial activity, possibly related to formation of microbialites. To date, onboard measurements have shown a certain degree of microbial activity, directly attached to mineral surfaces, which could be involved in microbialite formation. According to the activity measurements along the drill cores, the uppermost part, 0–4 meters below seafloor (mbsf) of the Tahiti reef environment, is the most active zone. This is a common trend in reef environments due the closeness to the photic zone inhabited by primary producing eukaryotes, such as algae. Pure microbiological activity was only observed in reef cavities where prokaryotic biofilms have appropriate conditions to develop (Figs. **F16, F17**).

Preliminary results show that the biofilms are diverse in structure and color. Figure **F16** shows an association between a brown iron/manganese crust and biofilm, whereas Figure **F17** shows an unusual a blue biofilm, which exhibited the highest degree of adenosine triphosphate (ATP) activity (20'600 RLU [relative light units]). In this sample, it was possible to define spherical assemblies of carbonate minerals embedded in the microbial exopolymeric substances (EPS). Figure **F18** shows 4,6-diamindino-2-phenylindole (DAPI)-stained cells in high densities in this biofilm in conjunction with mineral precipitation, which is most probably carbonate.

The biofilms appear to have high diversity in macroscale observations, and they are equally diverse and heterogenic in microscale resolution, as observed by scanning electron microscopy (SEM). Carbonate minerals appear in close relation with claylike

minerals (Fig. **F19;** Hole M0007C), carbonaceous microfossils (Fig. **F20;** Hole M0015B), and oxidized and reduced Fe minerals such as pyrite (Fig. **F21;** Hole M0023A). The metabolic processes responsible for the precipitation of this variety of minerals could not, as yet, be defined because of the complex and diverse conditions of the microenvironments where these biofilm were found.

Some evidence for heterotrophic metabolic activities is shown by exoenzyme measurements, which vary in the different biofilm samples. For instance, the samples from Holes M0020A (4.51 mbsf) and M0009D (3.64 mbsf) showed high phosphotase activity, suggesting a heterotrophic community that preferentially degrades organic bound phosphate compounds such as phospholipids or nucleic acids. In contrast, Hole M0007B (6.28 mbsf) showed only glucosidase and aminopeptidase activity, which is evidence for degradation and metabolization of polysaccharides and proteins.

Isolation of microorganisms from biofilm samples was performed on agar plates using a medium that is selective for heterotrophic bacteria. After 2 weeks incubation time, 10 different heterotrophic colonies could be isolated (Fig. **F22**). From anaerobic experiments, only one isolation was successful. Distinct groups of microorganisms are associated in the biofilm that could range from aerobic to anaerobic metabolism. SEM investigation of microbialite samples shows evidence that anaerobic conditions must have prevailed at times. The occurrence of framboidal pyrite well distributed in the sediment supports a certain degree of anoxia in the environment. Some sediment samples also show a close spatial association between the mineral phase and microbes (e.g., Figs. **F20, F23**).

As a biogeographical summary of microbial activity in the Tahiti reef, northwestern Faaa Hole M0020A and southwestern Maraa Holes M0005C, M0007B, M0007C, M0015B, and M0018A were more active than the northeastern Tiarei sites, where often no living biofilm could be detected in cavities along the core.

Geochemistry

Most importantly, interstitial water (IW) data from Expedition 310 demonstrate the ability to obtain geochemical signals (significant deviations from seawater chemistry) from fossil reef material. Rhizon sampling enabled IW samples to be taken where traditional whole-round squeezing was not possible and undesirable. For these reasons alone, the IW results from Expedition 310 are successful. The IW data indicate that

no significant contamination resulted from using seawater as the drilling fluid through the lack of ubiquitous metallic enrichments compared to Tahitian seawater. However, storage of samples in sealed glass vials following IODP tradition resulted in serious B and Si contamination of the samples upon opening of the vials. In the future, acid cleaned plastic bottles should be used to store IW samples.

General Remarks about Site M0008 Interstitial Water Data

Hole M0008A was drilled much more proximal to the island of Tahiti than any other sites and recovered volcanoclastic sediments. This made Hole M0008A unique compared to the other holes and offered opportunities to sample and analyze pore waters. In all the IW profiles, a barrier to diffusion is evident at ~18 mbsf, which corresponds to the position of a large basalt boulder recovered in Section 310-M0008A-8R-1. The lack of a chilled margin at the top and bottom of this basalt suggests it is not a continuous layer of basalt providing an impervious layer. However, the seismic profile used for site selection indicates a strong continuous reflector at approximately the same depth, suggesting the basalt may represent a continuous layer. Ultimately, with no recovery of Core 310-M0008A-7R above the basalt, the nature of the diffusion barrier will remain uncertain.

pH, Alkalinity, Ammonia, Chloride, and Sulfate

Above ~18 mbsf the pH of IW samples is similar to ambient seawater, but below the diffusion barrier pH decreases sharply with depth until the pore waters are slightly acidic (Fig. **F24A**). The IW alkalinity profile essentially traces that of pH (Fig. **F24B**). This increase in free H^+ ions results in an undersaturation of aragonite and calcite as calculated using PHREEQC (Parkhurst and Appelo, 1999) and shown in Figure **F24A.** Just below ~18 mbsf, significant amounts of ammonia are detected (Fig. **F24C**) indicating microbial activity. The ammonia appears to diffuse downward from this source just below the diffusion barrier. Chloride in the pore waters is essentially similar seawater with a slight depletion at the bottom of the section, precluding the influence of significant amounts of freshwater in these sediments. Sulfate concentrations do not significantly deviate from seawater values at any depth.

Mg, K, Ca, and Sr

There is no significant deviation of IW Mg concentration from that of seawater, whereas K becomes depleted with depth below the diffusion barrier at ~18 mbsf (Fig. **F24D**). Both Ca and Sr concentrations become highly elevated with depth below the

diffusion barrier (Fig. **F24E, F24F**), indicating dissolution of carbonate debris and/or weathering of the silicate material. The calculated undersaturation of calcite and aragonite in these pore waters suggests that carbonate dissolution must be contributing to these enrichments.

Li, P, Mn, Fe, and Ba

Li is depleted from seawater value (~174 µg/L) at all depths in Hole M0008A, suggesting Li uptake by clays in the siliclastic sediments (e.g., Zhang et al., 1998). P displays little variability with depth. Enrichment of the pore waters in Mn is observed in all samples from Hole M0008A, but there is an important source at ~20 mbsf below the diffusion barrier (Fig. **F24G**). Fe is greatly elevated in the IW samples from above the diffusion barrier at ~18 mbsf but was below detection in the samples from below the diffusion barrier (Fig. **F24H**). This pattern is interesting because conventional wisdom suggests that Mn oxide reduction occurs above the zone of Fe oxide reduction in marine sediments (e.g., Berner, 1980). One possible explanation for this pattern is that most Fe has already been lost from the older sediments below the diffusion barrier. However, iron oxide–rich sediments containing small root fragments indicative of a laterite soil were recovered in this interval of Fe-free pore waters. It is very interesting that Mn can be mobile in these sediments below the diffusion barrier and Fe is not. Ba is highly enriched in the pore waters below the diffusion barrier at ~18 mbsf, leading to a calculated barite oversaturation.

X-Ray Fluorescence

Five samples of volcanic sand/silt units and nine individual basalt samples were selected for bulk rock analysis by energy dispersive polarized X-ray fluorescence (EDP-XRF) analysis. All the samples analyzed by this technique were taken from Hole M0008A. Analytical results are shown in Table **T3.** The low SiO_2 but fairly high K_2O, P_2O_5, and TiO_2 contents (Na_2O was not analyzed) suggest that the volcanic rock samples belong to the alkalic basalt clan (i.e., alkalic basalt, basanite, tephrite, and nephelinite). The two texturally similar samples that apparently come from a single boulder show many compositional similarities, but they also have differences, especially with respect to MgO contents. The differences may be due to flow differentiation, which is known to create compositional variation within a lava flow, or to instrumental error. Two samples are fairly primitive (>14.0 wt% MgO and >350 ppm Ni), but one is highly olivine-pyroxene phyric, and thus its composition may have been compromised by crystal accumulation of the olivine and pyroxene. Despite their small number, the rock samples apparently show downhole compositional variation (Fig. **F25**).

Samples from the upper part of the hole have slightly higher incompatible element contents (e.g., K and Rb) but lower SiO_2 than those from the lower part of the hole, indicating that the shallow basalt samples are compositionally more alkalic than the deeper samples.

The volcaniclastic sand/silt samples are compositionally different from the whole rock basalt samples in that they have lower SiO_2 contents, which translates to lower total weight percent of all major oxides, obviously due to higher volatile contents, mainly seawater, as evidenced by their high Cl contents. Sulfur is also high in the sand/silt samples, particularly in the upper samples. The only rock sample that is high in both S and Cl is a scoriaceous pebble that probably contains a lot of pore water. Nevertheless, the upper sand/silt samples show many compositional similarities with the basalts, but the lower samples do not. The upper and lower sand/silt samples show apparent compositional differences (Fig. **F26**). Downhole compositional variations are observed in pore water chemistry, and thus the compositional differences between the upper and lower sand/silt units are probably real. Unlike the downhole compositional variation of the basalts, the sand/silt compositional differences are most probably due to differences in the depositional environment between the upper and lower volcanic sand/silt units.

Both Tahiti-Nui and Tahiti-Iti are composed predominantly of lava flows of moderately alkalic to strongly alkalic basalts; plutonic rocks are subordinate in amount and only exposed near their eroded centers (e.g., McBirney and Aoki, 1968; Cheng et al., 1993; Duncan et al., 1994). Differentiated rocks occur in subordinate amounts and were erupted mostly in the waning stages of volcanic activity. Thus, the lithologic composition of the volcaniclastic sediments drilled during Expedition 310, particularly the preponderance of lithic basalt clasts, unsurprisingly, is a direct reflection of the geology of the island. Compositionally, the rock samples and two upper sand/silt units plot with the rest of the igneous samples from Tahiti (Fig. **F27**). The two primitive basalts plot with the relatively fewer high-MgO basalts from Tahiti, whereas the other basalt samples plot with the more abundant, lower-MgO basalts. Many of the lower-MgO basalts in Tahiti can be modeled as crystal fractionation daughters of the higher-MgO parents (e.g., Cheng et al., 1993; Duncan et al., 1994). The two upper volcaniclastic sand/silt samples plot between the two basalt groups, either because their lithic basalt components are less fractionated than the lower-MgO basalts or they are similar to the latter but contain additional pyroxene mineral components. The three lower sand/silt samples generally plot outside the Tahiti lava field, suggesting that their compositions have been modified or altered.

PRELIMINARY SCIENTIFIC ASSESSMENT

During the Expedition 310 Onshore Science Party, emphasis was placed on visual description, measurement of physical properties, and sampling of the cores. Thus, the Expedition Report, scheduled to be published in March 2007, will contain a descriptive framework for the subsequent postcruise research.

The primary objectives of Expedition 310 require the use of specialized geochemical techniques, paleomagnetic analyses, and detailed investigation of lithological and biological assemblages. These types of analyses were not conducted during the Onshore Science Party but will be conducted over the coming months at the institutions of the Expedition Scientists as part of their postcruise research.

Fulfillment of the Expedition 310 scientific objectives is as follows:

1. *Establish the course of postglacial sea level rise at Tahiti (i.e., define the exact shape of the deglaciation curve for the period 20.00—10.00 ka.*

   During the offshore phase, cores were recovered from the postglacial reef sequence from 40 to 121 m below current sea level. Therefore, most if not all of the postglacial sequence from the LGM to the present day was recovered. During the Onshore Science Party, high-quality coral samples were taken for dating and sea level change investigations, the results of which are expected to fulfill the first objective.

2. *Define SST variations for the region over the period 20.00—10.00 ka.*

   During the offshore phase, massive coral colonies suitable for paleoclimate studies and spanning most of the postglacial sequence were recovered in the cores. During the Onshore Science Party, these massive coral colonies were slab-sampled for paleoclimate studies, the results of which are expected to fulfil the second objective.

3. *Analyze the impact of sea level changes on reef growth and geometry.*

   During the offshore phase, cores were recovered from holes in various water depths and situated on transects in three different areas around Tahiti. Therefore, results of analyses of samples taken during the Onshore Science Party will be interpreted in broad temporal and spacial contexts, which will allow better understanding of the development of the Tahiti reef.

OPERATIONS

Mobilization of the Hunter

Tampa, Florida

Mobilization of the drilling platform *Hunter* took place in two stages: the first stage was in Tampa, Florida (28 August–5 September 2005) and the second stage during the port call in Papeete, Tahiti (5–6 October 2005).

The first mobilization stage involved shipping of contractor drilling equipment and ESO laboratory and ancillary equipment to Tampa from Europe. After all the equipment had arrived and cleared customs, the vessel came on charter and was converted into a drilling vessel in just over 6 days. The Tampa Bay Shipyard Company provided port services, welders, and crane drivers. Seacore engineers carried out all engineering work, rig building, and certified the load testing of key structures. During the period of rig construction, ESO staff from the British Geological Survey (BGS) unloaded equipment from containers, set up a shipboard computer network, and connected power and water services to laboratories. They also made safe the walkways and core inspection areas on board with the drilling contractor. The ESO Operations Superintendent was also responsible for overseeing the entire load testing of key structural components of the rig. Verification of these milestone points was required to trigger contract stage payments. During this period of mobilization, we were pleased to receive a visit from Dr. Manik Talwani, President of IODP Management International Inc. (IODP-MI) and Dr. Jamie Allan of the U.S. National Science Foundation.

Transit to Papeete, Tahiti, with Brief Port Call in Panama

Mobilization work continued on passage to Panama (5–13 September 2005), where ESO personnel disembarked. Some Seacore personnel continued on the passage to Tahiti, completing mobilization activities en route (13 September–5 October).

Port Call in Papeete, Tahiti

The second stage of mobilization took place on 5–6 October 2005 during the port call in Papeete. Some air freight items for the expedition were taken on board during the port call; winches for logging and some equipment for the microbiology laboratory were loaded on deck. For this stage of mobilization, the complete ESO team was available. All laboratories and office spaces were networked with computers, the Drilling

Information System (DIS) database system was set up, onboard equipment was laid out, and a satellite-based e-mail system was installed.

At 0900 h on 6 October, the Expedition 310 Scientists joined the *Hunter*. A visit to the *Hunter* was arranged for local schoolchildren and the press for 1 h in the morning. By 1830 h, mobilization was complete and the vessel commenced day rate operations. The *Hunter* departed for the first site at 1930 h on 6 October, after spending 36 h in port.

Transit to Site M0005, Maraa

The *Hunter* arrived at Site M0005 at 2330 h on 6 October 2005 and immediately conducted dynamic positioning calibration tests ~250 m south of the first hole, M0005A. By 0250 h on 7 October, the vessel was positioned above Hole M0005A.

Site M0005

Hole M0005A

After overcoming problems with a hydraulic ram which caused the moonpool doors to fail to open, Seacore's Drilling and Reentry Template (DART) was deployed on American Petroleum Institute (API) drill string (used as conductor pipe for this expedition) to just above the seabed. From 1335 h on 6 October, a seabed survey around the position of the first site was conducted using the downpipe underwater camera. A suitable site was located ~2 m from the planned position, and the DART was placed on the seabed with 8 tonnes of weight. After removing the camera, the HQ (piggyback) drill string was run through the API conductor to the seabed, and coring operations in Hole M0005A commenced. The first core arrived on deck at 2000 h. Thereafter, coring continued with difficult barrel latching, and short core runs were used to avoid drilling rather than coring until the best coring parameters were established. The first cores displayed large cavities, and recovery was poor. Core barrel jams and problems with blocked bit–related mislatching led to slow progress in this hole. When reentering the hole after one particular drill string trip to remove a core blockage from the bit, coring appeared to recommence at 10.4 m. Good core was obtained, and it appeared that the borehole may have been restarted in a deviation or had avoided a previous deviation. This was taken as the start of a new hole, M0005B, at 1840 h on the 8 October.

Hole M0005B

At 0140 h on 9 October 2005 at 20 m depth, the core barrel failed to latch in. A replacement barrel also failed to latch. The hole was verified clear by the chisel tool. It was suspected that the HQ pipe was bent, and the string was tripped. On deck, the third and second pipe stands (four joints) of the HQ drill string were bent. The decision was made by all to terminate Hole M0005B, not to log, and make modifications to the DART before continuing with a new hole. The downpipe camera was prepared, and an environmental impact inspection of the coring area was carried out by raising the DART from the seabed and lowering the camera through the DART. There was difficulty in identifying the drilling area due to minimal impact of the DART on the seabed. The camera was recovered and the inspection was completed by 0615 h on 9 October.

Starting at 0615 h on 9 October, the API string was tripped and the DART was brought on deck and secured above moonpool. The vessel departed Site M0005 and headed for a nearby sheltered bay to carry out work on the DART. The DART feet were removed and a stinger was installed. The vessel departed the sheltered bay and was back at Site M0005 by 1330 h.

Hole M0005C

The *Hunter* took position above Hole M0005C, ~10 m east-southeast alongslope from Holes M0005A and M0005B, and was ready for operations by 1510 h on 9 October 2005. When lowering the DART on the API string, a burst hydraulic union on the rig hydraulics caused an operational shutdown until the oil spill on the deck was contained and repairs were made. At 1835 h, the downpipe underwater camera was deployed for a predrilling site check, and the stinger was engaged with the seabed under camera observation. The DART was drilled 1.3 m into seabed and stabilized ready for the coring string. The HQ coring string was run at 2000 h, and coring operations commenced in Hole M0005C. At 0545 h on 10 October, sand in the drill string caused the core barrel to jam and the string had to be tripped to free it. At 1110 h, the vessel requested a heading change, which was carried out with the HQ string off bottom but still in the hole. After the heading change, the core barrel was unable to be run into the HQ string and it was observed that the API pipe was not central in moonpool. The HQ string was tripped, and nine stands were removed with bends. A problem with the dynamic positioning system analyzed and resolved before resetting the DP to average the previous drilling position. At that position, the downpipe camera was run at 1515 h to see if the HQ hole was still in the stinger. No HQ hole was apparent, but

the decision was made to trip the HQ string with an insert bit and drill down to the previous depth. Reentry into the earlier borehole was not confirmed, even though the template had not moved, so a new hole (Hole M0005D) was started.

Hole M0005D

Coring commenced in Hole M0005D at 2330 h on 10 October 2005. Coring was steady and recovery moderate to good throughout the day on 11 October. At 0510 h on 12 October, the decision was made to stop coring in Hole M0005D after reaching 102 mbsf and without reaching the basaltic basement. The HQ string was pulled and the logging tools were prepared.

At 0750 h on 12 October, the DIL45 (electrical resistivity) tool was lowered but got stuck just below the seabed. It was suspected that the top of the hole was unstable, within a zone of low recovery noted while drilling. The top 5 m of the hole was cased with HQ pipe. The DIL45 tool was lowered but was still unable to enter the hole from the pipe. The HQ pipe was run all the way to the base of the hole, a spectral gamma log was run inside the HQ pipe, and then, after ensuring that the pipe was free from obstruction, the HQ pipe was pulled back in 25 m increments and logging was conducted in the open hole below the pipe.

Logging operations in Hole M0005D continued with excellent logs being obtained until the hole finally collapsed after pulling back the HQ pipe to 17 m below the seabed. The logging tools were in danger of becoming stuck in the top-hole section and were retrieved. After a heading change, the remaining HQ pipe was pulled, the DART was lifted, and operations in Hole M0005D ceased at 1310 h on 13 October. A post-drilling seabed survey using the downpipe camera was conducted before leaving the hole.

Hole M0005E

Before departing Site M0005, four hammer samples were taken in Hole M0005E (~5 m alongslope from Hole M0005D in 61.34 m water depth). Four samples were taken to a depth of 2 m below seabed, with typically 80% recovery. After curation, these samples were handed to the microbiologists to sample at will, before the remainder was passed to the sedimentologists and coral specialists for description. Operations in Hole M0005E were concluded by 1635 h on 13 October 2005. Before progressing to the next site, the *Hunter* conducted a 360˚ maneuver to verify that positioning offsets at the drill string were zero.

Site M0006

A move to deeper water (~80 m) was undertaken, and the *Hunter* was repositioned above Hole M0006A in 81.58 m water depth. Another four hammer samples were collected, primarily for microbiology, before the drill string was lowered onto what appeared to be a very steep slope. Both the ship's transponder and tautwire indicated that they were sliding downslope and suggested that the bathymetric data were insufficient to allow a reasonable picture of the seabed. Any slope instability may have led to the DART sliding away downslope, and the decision was made to avoid the outer reef edge until either more seabed information was obtained or modifications were made to the DART to allow greater stability on steep slopes. Site M0006 was departed at 2300 h on 13 October 2005.

Site M0007

Hole M0007A

Hole M0007A was located farther back from the reef edge than Sites M0005 and M0006, in 44.45 m water depth. The seabed was surveyed using the downpipe camera, and at 0330 h on 14 October 2005, four hammer samples were taken. After hammer sampling, the HQ string was run and rotary coring commenced in the same hole. Coring continued with good recovery for the rest of the day. Total depth (TD; 44.4 m) was reached at 0120 h on 15 October.

Prior to tripping the HQ pipe, the gamma tool was run inside the pipe. Logging results from Hole M0005D indicated that the shape of the gamma trace through the pipe, when scaled accordingly, did not differ significantly when compared to the open hole trace, although statistically the results are less useful. After gamma logging, the HQ pipe was tripped, the core barrel removed, and the string rerun with a casing shoe to 7.5 m below seabed. Open hole logging commenced from TD to the casing shoe. After running the resistivity and hydrochemical tools in the open hole section, the acoustic imaging tool would not progress much beyond the casing shoe, despite being run with a sinker bar. Logging was terminated in Hole M0007A at 0700 h on 15 October.

Hole M0007B

After a postdrilling seabed survey using the downpipe camera, the *Hunter* moved 50 m alongslope to Hole M0007B. Two hammer samples were collected before rotary coring commenced in the same hole. Core recovery was poor in the top part of the

hole, and the coring parameters were checked for any changes that may have been responsible. Zero bit weight and high rates of penetration confirmed that an open structure was being drilled. The formation became more compact with depth, and recovery improved accordingly. Coring continued until 0630 h on 16 October 2005.

The HQ pipe was tripped and a casing shoe fitted before the pipe was rerun to the base of the hole for in-pipe gamma logging. After gamma logging, the HQ pipe was pulled to 24.6 m below seabed, and resistivity, hydrochemical, acoustic imaging, and optical imaging tools were run. It was not possible to log the entire bottom-hole section due to hole blockage (below 30 m below seabed). Logging in Hole M0007B was completed by 1410 h on 16 October. The remainder of the HQ pipe was pulled, and a seabed survey using the downpipe camera was conducted. The survey showed that the DART had been drilled well into the seabed (1.5 m) and had left a shallow debris-filled depression. However, the surrounding seabed showed minimal disturbance from the drilling. The DART was then lifted onto the deck through the moonpool and secured.

Transit from Site M0007 (Maraa) to Site M0008 (Tiarei)

At 1700 h on 16 October 2005, the vessel departed Site M0007 and headed for Site M0008, located on transect TAH-02A off the northeast coast of Tahiti, arriving at 2400 h.

Site M0008

Shortly after arrival at 2400 h, a seabed survey using the downpipe camera was conducted. At 0400 h on 17 October 2005, coring operations began in Hole M0008A. This hole was to serve as a reference hole for the other holes on the transect. However, the material recovered consisted of river deposits of unconsolidated basalt gravel and pebbles mixed with volcaniclastic sediments. As a result, recovery was poor throughout (24.5%). TD was reached at 40.2 m below seabed, and operations ended in Hole M0008A at 1720 h on 17 October.

Site M0009

Hole M0009A

An assessment was made of where to drill next, in light of the results obtained in Hole M0008A. It was decided to attempt to drill the pinnacle at proposed Site TAH-02A, #4 on seismic Profile SISM 079. Acknowledging that the feature imaged on the seismic

line may be the result of sideswipe and may possibly be located off the seismic line, a localized search was made for a suitable drilling location using the ship's echo sounder and the tautwire to detect a shallower than expected water depth. No suitable position was located, and at 2100 h on 17 October 2005, the vessel was positioned above a flat terrace (Hole M0009A) nearby and drilling operations commenced and continued until 1915 h on 18 October. Recovery was moderate to poor (43.1%) to TD of 23.04 m below seabed. However, promising coral material was recovered and it was decided to attempt to recover the same section in a new hole nearby. By 2000 h, the HQ pipe had been recovered and the DART lifted off the seabed, and by 2015 h the vessel was positioned above Hole M0009B, ~5 m downslope from Hole M0009A. Coring operations commenced and continued until 1200 h on 19 October, with an improved recovery of 66.26%.

Hole M0009B

Prior to logging Hole M0009B, the hole was reamed. Logging began at 1530 h on 19 October 2005 with the resistivity and hydrochemical tools run in open hole over the interval 6–21 m below seabed. A hole blockage near the postglacial/Pleistocene boundary, which resisted attempts to clear with the chisel tool, prevented the tools from being run below ~21 m below seabed. Optical image logs were collected from 6 to 18.1 m below seabed, and acoustic image logs were collected between 6 and 13.8 m below seabed. Logging of Hole M0009B was concluded by 2320 h on 19 October.

Hole M0009C

Just before 0000 h on 20 October 2005, the *Hunter* moved to Hole M0009C, ~9 m west-northwest of Hole M0009B in 99.85 m water depth. Coring commenced and continued until 1935 h that day, reaching a TD of 25.66 m. Coring in Hole M0009C proved very difficult, with many bit blockages and crushed liners resulting from pieces of the formation breaking off and entering the core barrel, having not been properly cored. The lattice drilled was not strong enough to core and, in many cases, had to be crushed for progress to be made. Recovery improved toward the base of the hole, and the total core recovery was 51.86%. At 1935 h, the hole was completed and preparations made to move to Hole M0009D.

Hole M0009D

The *Hunter* was positioned above Hole M0009D, 5.5 m east of Hole M0009B in 103.18 m water depth, and coring began at 2210 h on 20 October 2005. Coring in Hole

M0009D continued until 2230 h on 21 October to a TD of 44.59 m. Progress was steady, but core runs were short and bit blocking common. After TD was reached, preparations were made to log the hole.

Prior to logging the hole, the hole was reamed and flushed for 30 min. The HQ string was pulled and set with a casing shoe at 19 m below seabed to run the logging tools through the open hole section. Logging commenced at 2230 h on 21 October in very wet and windy conditions. This, combined with very poor hole conditions, led to a difficult logging period. Nevertheless, good logs were obtained in sections of open hole where it was possible to log. A hole blockage prevented the resistivity tool from reaching the base of the hole, and the chisel tool was used to clear the blockage. The resistivity, spectral gamma ray, and acoustic tools were run. However, large, meter-scale cavities in the formation created sticking points for some of the tools; thus, only some of the open bottom-hole interval was logged. The first optical image tool run was affected by power failures on the drill rig, possibly caused by very heavy rainfall. Logging was temporarily interrupted while the cause of the power failures was investigated. After these runs, the casing was pulled to 5 m below seabed. The top-hole section was logged with the resistivity and optical image tools, with cavities causing problems for the optical tool. While logging uphole, the optical image tool became stuck many times and needed to be pulled through obstructions by hand. Logging operations were completed by 1000 h on 22 October, and preparations were made to move to Hole M0010A.

Site M0010

The *Hunter* was positioned above Hole M0010A by 1400 h on 22 October 2005, ~140 m east-southeast of proposed Site TAH-02A, #4 in 89.53 m water depth. The DART was drilled into the seabed, and coring operations began at 1635 h. Coring continued until 1000 h on 23 October to a TD of 34.6 m below seabed. During the coring period, an HQ string trip was made to clear a continually blocking bit.

Site M0011

Hole M0011A was located ~140 m east of proposed Site TAH-02A, #4 in 101.34 m water depth. After running the API pipe, drilling the DART into the seabed, and running the HQ pipe, coring operations began at 1330 h on 23 October 2005. Coring commenced in very soft silts with poor recovery, but this improved when the river depos-

its gave way to a carbonate framework. At 0030 h on 24 October, coring operations were completed in Hole M0011A at a depth of 17.65 m below seabed.

Site M0012

Hole M0012A was the first of three holes to be located within the new EPSP-approved zone southeast of proposed Site TAH-02A, #4. Before the DART was lowered onto the seabed, a downpipe camera survey was run which showed a live coral colony at the first location. The ship was repositioned 25 m downslope in 77.05 m water depth, and the DART drilled in. Coring operations began om Hole M0012A at 0900 h on 24 October 2005. Recovery was generally poor, although it did improve in the more competent material at the base of the hole. Coring was completed at 2040 h on 24 October at a TD of 34.1 m.

Site M0013

Hole M0013A was located 30 m downslope from Hole M0012A, in 90.95 m water depth. The *Hunter* was positioned above the hole at 2300 h on 24 October 2005. After the API pipe and DART were lowered to the seabed, a seabed camera survey was conducted. Coring operations began at 0100 h on 25 October. At 0415 h, coring was abandoned due to the lack of suitable coral material. TD of the hole was 11.7 m.

Site M0014

Hole M0014A was spudded ~70 m north-northwest of Hole M0013A in 99.25 m water depth. Coring operations began at 0610 h on 25 October 2005 and were completed at 1615 h at a TD of 15.43 m. The HQ string, API pipe, and DART were lifted onto deck and secured for the transit to previous Site M0007 at the south end of the island.

Transit from Site M0014 (Tiarei) to Site M0007 (Maraa)

Poor weather was forecast for north of the island, and so the decision was made to revisit promising sites in the south. The transit commenced at 1930 h, and Site M0007 reached at 0200 h on 26 October 2005.

Site M0007

Hole M0007C

Prior to coring Hole M0007C, a seabed camera survey was conducted which revealed a surprisingly barren sloping seabed in 43.35 m water depth. Coring operations began at 0315 h and continued until 2215 h. The hole progressed quickly, with core recovery generally poor and little formation resistance being evident on the bit. At ~30 m below seabed, the hole started to become sticky and then collapsed during a wireline trip, filling the outer core barrel with cuttings. The string was tripped, the barrel cleaned out (2 m of coral cuttings), and the HQ string rerun with an insert bit as the inner core barrel. The base of the hole was reached with difficulty, where rotation also became difficult. The string stuck a few times, and the hole was abandoned at a TD of 32.25 m.

Site M0015

After completing Hole M0007C, ~300 m to the northwest, the *Hunter* moved to Site M0015 in 72.15 m of water. After a short bathymetry traverse to locate a site for the hole, drilling operations began at 0030 h on 27 October 2005 and continued until 0325 h on 28 October. TD was 42.28 mbsf. There was generally good core recovery, with usually <1 m core runs between bit blocking and 72.71% average recovery for the hole.

Prior to logging, Hole M0015A was reamed and flushed for 1 h, after which the core barrel was removed and the drill string rerun with a casing shoe. Logging commenced at 0630 h on 28 October. Initially, the casing depth was set at 7 m but the logging tools would not pass downhole beyond 20 m, so they were removed and the casing run to the base of the hole then pulled back to 20 m. Logging then was possible in the bottom part of the borehole, but one tool was stuck for a while and had to be eased free with the downhole hammer. Thereafter, logging continued successfully, the casing was pulled back to 7 m, and the remainder of the hole logged with overlap. Logging operations in Hole M0015A were completed by 1930 h on 28 October. The string was then tripped to deck and the DART lifted off seabed.

Site M0016

Hole M0016A

After moving to new Site M0016, a tautwire bathymetry traverse was conducted to locate a site for Hole M0016A. By 2400 h on 28 October 2005, the *Hunter* was positioned above Hole M0016A in 80 m water depth. Shortly after midnight on 29 October, coring operations began. Throughout the day, coring continued with fairly poor recovery, and drilling indicated that the formation had many cavities. Coring in Hole M0016A was terminated at 0620 h on 30 October at a TD of 38.31 m. This was due to difficulty in overcoming bit blocking and, after a string trip to clean the whole core barrel system, the HQ inner barrel could not reenter the outer pipe because to the string was bending. It is most likely that the DART had moved on the seabed, possibly through subsidence.

Hole M0016B

Hole M0016B was located 5 m east of Hole M0016A. Initially, the noncoring insert bit was used to drill to 17 m below seabed and then coring continued with variable but generally good core recovery. Coring operations ended at 0230 h on 31 October 2005 at a TD of 44.62 m.

Site M0006 (Survey)

After moving to previous Site M0006, a tautwire site survey was conducted along a short transect. This survey was abandoned after the DART touched down on the seabed unexpectedly, indicating that the bathymetry for this area was not accurate. After running the downpipe camera to check for stinger damage and lifting the DART higher from the seabed, a new tautwire survey was conducted 10 m east of the previous transect. A suitable site was found, but when the DART was lowered it touched the seabed 2 m deeper than indicated by the tautwire. The topography of the seafloor was suspected to be very uneven at this survey location, so a new survey transect was initiated 10 m to the east. During this survey, the DART unexpectedly touched seabed again. The seabed depth at Site M0006 appeared to change rapidly, and the changes were not evident on the bathymetry data. Therefore the search for a new site was abandoned, the DART lifted into the moonpool, and the *Hunter* returned to previous Site M0015.

Site M0015

Hole M0015B

The *Hunter* moved back to previous Site M0015 to start new Hole M0015B in 71.53 m water depth. Coring operations began at 1330 h on 31 October 2005 and were completed by 1730 h on 1 November at a TD of 40.12 m. Because very short core runs were being achieved in the lower part of the hole and most liners were being crushed, the last four or five runs were made using the split chromed steel liners commonly used elsewhere for this type of coring. The immediate result was longer core runs before jamming, better core recovery, and improved preservation of delicate structures. Some horizons which would previously have been crushed were kept intact or kept in their correct cored position.

Site M0017

Hole M0017A was located ~60 m north of Hole M0015B in 56.5 m water depth. Before touching down with the DART, a seabed camera survey was run to check for living corals. None were observed, and so coring operations began at 2300 h on 1 November 2005. A faster penetration rate was achieved using the steel split liners, giving the drillers a much more sensitive indicator of bit blocking. As a consequence, they were able to detect bit blocking much quicker and were sometimes able to avoid it. This meant that the core runs were longer and the number of wireline trips reduced. Core recovery also improved. No problems were encountered with the subsequent curation or science through the use of steel split liners. Coring was completed by 1600 h on 2 November at a TD of 40.56 m.

Prior to logging Hole M0017A, the hole was flushed. There was some difficulty with a stuck HQ pipe while trying to trip the drill string, which could be rotated but not uplifted. The string eventually came free. A casing shoe was fitted for the logging operation. Logging commenced in Hole M0017A at 2130 h on 2 November and was completed by 0350 h on 3 November. Resistivity, acoustic imaging, optical imaging, hydrochemical, caliper, and sonic tools were run. The starting depth of the tools varied because the tools caught in cavities (between 31.55 and 23.23 mbsf) and the depth of the casing pipe was 13.35 mbsf. The core barrel fishing cable was used on one occasion to pull the sonic tool, which was stuck just below the casing, up to the surface. This process damaged a portion of the logging winch cable, which was cut at ~85 m. Reheading of the winch cable was completed well before the next logging operation.

Site M0018

A short echo sounder survey (30 m × 20 m grid) was conducted ~120 m south-southeast of proposed Site TAH-03A-1 to locate a suitable site for Hole M0018A. At 0915 h on 3 November 2005, the DART was lowered at the chosen site and touched the seabed 14 m deeper than suggested by the echo sounder survey. The specific site was resurveyed using the lead-line, and a new site chosen nearby. The DART was unable to be drilled-in at this site at first (a solid carbonate crust was evident on the camera survey) but was successfully drilled in on the second attempt (after the crust was broken by the stinger?). At 1640 h on 3 November, coring operations began in Hole M0018A and continued until 1200 h on 4 November. TD of the hole was 40.05 mbsf, with a total recovery of 61.50%. The nature and quality of the material collected indicated that most of the coreable material was being collected. A camera survey was conducted after withdrawing the drilling equipment from the hole. No undue disturbance was observed, although there was a significant mound where the DART was situated with a slight "tail" of (?)cuttings coming from it and going down the presumed slope.

Transit from SIte M0018 (Maraa) to Site M0019 (Faaa)

Prior to departing the Maraa area, the tautwire was respooled and the DART lifted onto the deck of the *Hunter* and secured. Once on deck, the stinger below the DART was found to be missing, and a new stinger was fitted. The vessel departed the Maraa area at 1750 h on 4 November 2005 and arrived at the Faaa area at 2030 h.

Site M0019

On arrival at Faaa, the *Hunter* was positioned above Hole M0019A (~31 m south of proposed Site TAH-01A, #3) in 58 m water depth. All clearances with airport and seaport authorities were double-checked before occupying the new location, which was closest to the visible reef so far. A seabed camera survey was run, and no live corals were observed. The DART was lowered and drilled in, and coring operations in Hole M0019A began at 2320 h on 4 November 2005. Coring was completed at 2400 h on 5 November at a TD of 66.96 mbsf and with a total recovery of 41.12%. Penetration was rapid but recovery was poor. Checks of the Jean Lutz automatic drilling recorder data confirmed the driller's view that there were significant void spaces throughout. When penetration rate reduced to below 10 m/h, indicating more solid material, core was usually obtained.

Site M0020

Prior to coring Hole M0020A, the DART was retrieved and a short echo sounder survey was conducted 50 m north of Hole M0019A to locate a site for Hole M0020A. The chosen site was checked using the tautwire, and the DART and drill pipe were deployed in 83 m water depth. Coring operations began in Hole M0020A at 1200 h on 6 November 2005 and continued until 1220 h on 7 November to a TD of 42.16 m. Total recovery was 70.45%.

Transit from Site M0020 (Faaa area) to Site M0021 (Tiarei area)

The vessel departed the Faaa area at 1320 h on 7 November 2005 and arrived in the Tiarei area at 1610 h.

Site M0021

An echo sounder survey (five profiles) was conducted over suspected drowned reefs near to the foreslope imaged on the bathymetry. The water depth was confirmed at two locations using the tautwire. After a seabed camera survey, the DART was drilled in at one of these locations, ~115 m southeast of proposed Site TAH-02A, #5 in 82 m water depth. Coring operations began in Hole M0021A at 2200 h on 7 November 2005 and continued until 1640 h on 8 November. TD was 34.23 mbsf and total recovery was 74.87%. Good core recovery confirmed that the submerged pinnacle is a drowned reef.

Site M0009

Hole M0009E

After coring in Hole M0021A was completed, the HQ pipe was lifted and the DART raised to 45 mbsl. The vessel moved 90 m northwest to previous Site M0009, where a site for Hole M0009E was chosen in a water depth of 93 m. The DART was lowered and drilled in, and coring operations in Hole M0009E began at 2030 h on 8 November 2005. Coring was completed at 0550 h on 9 November at a TD of 20.61 m and with a total recovery of 72.73%.

Prior to logging, the hole was flushed and the HQ pipe pulled and rerun with a casing shoe. From 0715 h on 9 November, Hole M0009E was logged between ~2 and 15 m below the seabed. The chisel tool was deployed once to clear a blockage at 6 mbsf.

After logging was completed at 1440 h, the HQ pipe was tripped and the DART raised into mid-water.

Site M0022

The *Hunter* was positioned above Hole M0022A, ~175 m north-northwest of proposed Site TAH-02A-4 in 115 m water depth. After checking the depth with the tautwire, the DART was drilled in and coring commenced at 1750 h on 9 November 2005. It was hoped that the hole would penetrate a Pleistocene gulley which may been subsequently accreted by postglacial corals. Basalt gravel and volcaniclastic sand of Pleistocene affinity were recovered from a shallow depth, and so Hole M0022A was abandoned after 8.8 m penetration at 2310 h on 9 November. By midnight, preparations were being made to trip the API pipe and DART.

Site M0023

Hole M0023A

From 0000 h on 10 November 2005, the DART was raised to the moonpool after abandoning coring in Hole M0022A. The *Hunter* moved to a new area over a drowned reef to conduct an echo sounder survey, ~100 m southwest of proposed Site TAH-02A, #4. From 0200 h on 10 November, 9 m × ~110 m echo sounder traverses were made over the drowned reef pinnacle, from which a site for Hole M0023A was chosen in 67 m water depth. After a short camera survey, coring operations in Hole M0023A started at 0635 h on 10 November and ended at 2245 h that day after reaching a TD of 31.36 mbsf with a total recovery of 77.20%.

Hole M0023B

After raising the DART a short distance from the seabed, the *Hunter* was positioned above Hole M0023B, 5 m southwest of the previous hole in 67 m water depth. Coring operations in Hole M0023B began at 0120 h on 11 November 2005 and ended at 1540 h that day at a TD of 31.12 mbsf with a total recovery of 67.90%. The coring operation proceeded smoothly, with excellent core recovery in long core runs in often very porous formation.

Prior to logging, the drill pipe was pulled and the hole flushed to 30 min before the drill pipe was run-in with a casing shoe to ~6 mbsf. Logging commenced at 1700 h on 11 November. Initially, the tools would not pass below the casing shoe, even after

the chisel tool was worked in the hole. The casing shoe was run to the base of the hole and back before the chisel tool was deployed to check that the casing shoe was clear. Logging operations restarted at 2000 h, with the tools reaching a maximum depth of 28.5 mbsf. A DP malfunction caused the vessel to move off location during logging, but the situation was recovered and the hole and equipment remained intact. The optical and acoustic log preview indicated that there were many cavities in the formation. Logging was completed in Hole M0023B at 0310 h on 12 November.

Site M0024

After clearing away the logging tools and lifting the DART back into the moonpool, the vessel moved to conduct an echo sounder survey in an area over a drowned reef pinnacle ~100 m east of proposed Site TAH-02A, #5. From 0515 h on 12 November 2005, 14 m × 50 m echo sounder traverses were made, from which a site for Hole M0024A was chosen in 90 m water depth. Coring operations in Hole M0024A began at 1010 h on 12 November and finished at 0400 h on 13 November at a TD of 32.3 mbsf. Total recovery was 83.74%.

Site M0025

Hole M0025A

A site for Hole M0025A was chosen from the echo sounder survey conducted on 12 November 2005, 25 m north-northwest of Hole M0024A. The DART touched down in a water depth of 105.4 m and coring began at 0530 h on 13 November and finished at 1645 h that day at a TD of 20.93 mbsf. Total recovery was 74.23%.

Site M0026

Following another echo sounder survey over a 50 m × 35 m area ~180 m east of proposed Site TAH-02A, #4 over a drowned reef pinnacle, a site for Hole M0026A was chosen. It proved difficult to interpret the results of the echo sounder survey (three strong seabed echoes and widely differing water depths over a few meters), and it took some time before identifying a suitable site in 105 m water depth. Coring operations in Hole M0026A started at 0920 h on 14 November 2005 and were completed by 1105 h that day at a TD of 12.4 mbsf. Total recovery was 58.45%.

Site M0025

Hole M0025B

After lifting the DART from Hole M0026A, the *Hunter* moved to previous Site M0025 to core Hole M0025B. After taking a tautwire depth of 95 m, the DART was lowered and coring began at 1215 h on 14 November 2005. Coring finished at 0100 h on 15 November at a TD of 20.5 mbsf with a total recovery of 71.19%.

Site M0021

Hole M0021B

After raising the DART to 50 m above seabed, the vessel was moved back to Site M0021 to core Hole M0021B. Once on position, the tautwire depth was taken as 80 m. The DART and drill pipe were lowered, and coring in Hole M0021B commenced at 0630 h on 15 November 2005 and continued until 2210 h that day. TD was 32.81 mbsf and the total recovery was 65.57%.

Prior to logging, the hole was flushed before the HQ pipe was run back into the hole with a casing shoe. Logging of Hole M0021B commenced at 0030 h on 16 November and was competed by 0645 h that day. All tools were run to 15 mbsf. Once logging was completed, the DART was lifted onto deck and secured for the transit back to the Port of Papeete.

Transit to Port of Papeete

The *Hunter* departed the last site at 0815 h on 16 November 2005 and arrived at the Port of Papeete at 1145 h. Demobilization of the vessel took place on 16–17 November 2005.

Onshore Science Party, Bremen

The cores collected offshore Tahiti were transported under refrigeration to the new IODP Bremen Core Repository and Laboratories in the MARUM building on the campus of Bremen University. Further analytical laboratories were accessed through the Department of Geosciences (geochemistry laboratories), the Research Center for Ocean Margins (RCOM) (physical property laboratories), and the Centre for Marine Environmental Research (MARUM) of Bremen University. During the Expedition 310

onshore science party (13 February–4 March 2006), the cores were described in detail ad minimum and some standard measurements were made (Table **T2**).

REFERENCES

Anderson, D.M., and Webb, R.S., 1994. Ice-age tropics revisited. *Nature (London, U. K.),* 367:23–24. **doi:10.1038/367023a0**

Bard, E., Hamelin, B., Arnold, M., Montaggioni, L., Cabioch, G., Faure, G., and Rougerie, F., 1996. Deglacial sea-level record from Tahiti corals and the timing of global meltwater discharge. *Nature (London, U. K.),* 382:241–244. **doi:10.1038/382241a0**

Bard, E., Hamelin, B., and Fairbanks, R.G., 1990a. U-Th ages obtained by mass spectrometry in corals from Barbados: sea level during the past 130,000 years. *Nature (London, U. K.),* 346:456–458. **doi:10.1038/346456a0**

Bard, E., Hamelin, B., Fairbanks, R.G., and Zindler, A., 1990b. Calibration of the ^{14}C timescale over the past 30,000 years using mass spectrometric U-Th ages from Barbados corals. *Nature (London, U. K.),* 345:405–410. **doi:10.1038/345405a0**

Bard, E., Rostek, F., and Sonzogni, C., 1997. Interhemispheric synchrony of the last deglaciation inferred from alkenone palaeothermometry. *Nature (London, U. K.),* 385:707–710. **doi:10.1038/385707a0**

Beck, J.W., Récy, J., Taylor, F., Edwards, R.L., and Cabioch, G., 1997. Abrupt changes in early Holocene tropical sea surface temperature derived from coral records. *Nature (London, U. K.),* 385:705–707. **doi:10.1038/385705a0**

Berner, R.A., 1980. *Early Diagenesis: A Theoretical Approach:* Princeton, NJ (Princeton Univ. Press).

Blanchon, P., and Shaw, J., 1995. Reef drowning during the last deglaciation: evidence for catastrophic sea-level rise and ice-sheet collapse. *Geology,* 23(1):4–8. **doi: 10.1130/0091-7613(1995)023<0004:RDDTLD>2.3.CO;2**

Broecker, W.S., 1990. Salinity history of the Northern Atlantic during the last deglaciation. *Paleoceanography,* 5:459–467.

Broecker, W.S., 1992. Defining the boundaries of the late glacial isotope episodes. *Quat. Res.,* 38:135.

Camoin, G.F., Colonna, M., Montaggioni, L.F., Casanova, J., Faure, G., and Thomassin, B.A., 1997. Holocene sea level changes and reef development in the southwestern Indian Ocean. *Coral Reefs,* 16(4):247–259. **doi:10.1007/s003380050080**

Chappell, J., and Polach, H., 1991. Post-glacial sea-level rise from a coral record at Huon Peninsula, Papua New Guinea. *Nature (London, U. K.),* 349:147–149. **doi:10.1038/349147a0**

Cheng, Q.C., Macdougall, J.D., and Lugmair, G.W., 1993. Geochemical studies of Tahiti, Teahitia and Mehetia, Society Island chain. *J. Volcanol. Geotherm. Res.,* 55(1–2):155–184. **doi:10.1016/0377-0273(93)90096-A**

Dullo, W.C., Camoin, G.F., Blomeier, D., Colonna, M., Eisenhauer, A., Faure, G., Casanova, J., and Thomassin, B.A., 1998. Morphology and sediments of the fore-slopes of Mayotte, Comoro Islands: direct observations from a submersible. *In* Camoin, G.F., and Davies, P.J., *Reefs and Carbonate Platforms in the Pacific and Indian Oceans:* Oxford (Blackwell), 219–236.

Duncan, R.A., Fisk, M.R., White, W.M., and Neilsen, R.L., 1994. Tahiti: geochemical evolution of a French Polynesian volcano. *J. Geophys. Res.,* 99(B12):24341–24358. **doi:10.1029/94JB00991**

Edwards, R.L., Beck, J.W., Burr, G.S., Donahue, D.J., Chappell, J.M.A., Bloom, A.L., Druffel, E.R.M., and Taylor, F.W., 1993. A large drop in atmospheric $^{14}C/^{12}C$ and reduced melting in the Younger Dryas, documented with ^{230}Th ages of coral. *Science,* 260:962–968.

Fairbanks, R.G., 1989. A 17,000-year glacio-eustatic sea level record: influence of glacial melting rates on the Younger Dryas event and deep-ocean circulation. *Nature (London, U. K.),* 342:637–642. **doi:10.1038/342637a0**

Fleming, K., Johnston, P., Zwartz, D., Yoyoyama, Y., Lambeck, K., and Chapell, J., 1998. Refining the eustatic sea-level curve since the Last Glacial Maximum using far-and intermediate-field sites. *Earth Planet. Sci. Lett.,* 163(1–4):327–342. **doi:10.1016/S0012-821X(98)00198-8**

Gagan, M.K., Ayliffe, L.K., Hopley, D., Cali, J.A., Mortimer, G.E., Chappell, J., McCulloch, M.T., and Head, M.J., 1998. Temperature and surface-ocean water balance of the mid-Holocene tropical western Pacific. *Science,* 279:1014–1018. **doi:10.1126/science.279.5353.1014**

Grammer, G.M., and Ginsburg, R.N., 1992. Highstand versus lowstand deposition on carbonate platform margins: insight from Quaternary foreslopes in the Bahamas. *Mar. Geol.,* 103(1–3):125–136. **doi:10.1016/0025-3227(92)90012-7**

Grootes, P.M., Stuiver, M., White, J.W.C., Johnsen, S., and Jouzel, J., 1993. Comparison of oxygen isotope records from the GISP2 and GRIP Greenland ice cores. *Nature (London, U. K.),* 366:552–554. **doi:10.1038/366552a0**

Guilderson, T.P., Fairbanks, R.G., and Rubenstone, J.L., 1994. Tropical temperature variations since 20,000 years ago: modulating interhemispheric climate change. *Science,* 263:663–665.

Johnsen, S.J., Clausen, H.B., Dansgaard, W., Fuhrer, K., Gundestrup, N., Hammer, C.U., Iversen, P., Jouzel, J., Stauffer, B., and Steffensen, J.P., 1992. Irregular glacial interstadials recorded in a new Greenland ice core. *Nature (London, U. K.),* 359:311–313. **doi:10.1038/359311a0**

Lambeck, K., 1993. Glacial rebound and sea-level change: an example of a relationship between mantle and surface processes. *In* Wortel, M.J.R., Hansen, U., and Sabadini, R. (Eds.), *Relationships between Mantle Processes and Geologic Processes at or near the Earth's Surface:* Amsterdam (Elsevier), 15–37.

Lindstrom, D.R., and MacAyeal, D.R., 1993. Death of an ice sheet. *Nature (London, U. K.),* 365:214–215. **doi:10.1038/365214a0**

Locker, S.D., Hine, A.C., Tedesco, L.P., and Shinn, E.A., 1996. Magnitude and timing of episodic sea-level rise during the last deglaciation. *Geology,* 24:827–830. **doi:10.1130/0091-7613(1996)024<0827:MATOES>2.3.CO;2**

Macintyre, I.G., Rützler, K., Norris, J.N., Smith, K.P., Cairns, S.D., Bucher, K.E., and Steneck, R.S., 1991. An early Holocene reef in the western Atlantic: submersible investigations of a deep relict reef off the west coast of Barbados, W.I. *Coral Reefs,* 10(3):167–174. **doi:10.1007/BF00572177**

McBirney, A.R., and Aoki, K., 1968. Petrology of the island of Tahiti. *Mem.—Geol. Soc. Am.,* 116:523–556.

McCulloch, M., Mortimer, G., Esat, T., Xianhua, L., Pillans, B., and Chappell, J., 1996. High resolution windows into early Holocene climate: Sr/Ca coral records from the Huon Peninsula: *Earth Planet. Sci. Lett.,* 138(1–4):169–178. **doi:10.1016/0012-821X(95)00230-A**

McCulloch, M.T., Tudhope, A.W., Esat, T.M., Mortimer, G.E., Chappell, J., Pillans, B., Chivas, A.R., and Omura, A., 1999. Coral record of equatorial sea-surface temperatures during the penultimate deglaciation at Huon Peninsula. *Science,* 283:202–204. **doi:10.1126/science.283.5399.202**

Okuno, J., and Nakada, M., 1999. Total volume and temporal variation of meltwater from Last Glacial Maximum inferred from sea-level observations at Barbados and Tahiti. *Palaeogeogr., Palaeoclimatol., Palaeoecol.,* 146(1–4):283–293. **doi:10.1016/S0031-0182(98)00136-9**

Parkhurst, D.L., and Appelo, C.A.J., 1999. User's guide to PHREEQC (version 2)—a computer program for speciation, batch-reaction, one-dimensional transport and inverse geochemical calculations. Water-Resour. Invest. Rep. (U.S. Geol. Surv.), 99–259.

Peltier, W.R., 1994. Ice age paleotopography. *Science,* 265:195–201.

Raymer, L.L., Hunt, E.R., and Gardner, J.S., 1980. An improved transit-to-porosity transform. *SPWLA 21 Ann. Logging Symp.:* 1–12.

Rind, D., and Peteet, D., 1985. Terrestrial conditions at the Last Glacial Maximum and CLIMAP sea-surface temperature estimates: are they consistent? *Quat. Res.,* 24:1–22. **doi:10.1016/0033-5894(85)90080-8**

Stocker, T.F., and Wright, D.G., 1991. Rapid transitions of the ocean's deep circulation induced by changes in surface water fluxes. *Nature (London, U. K.),* 351:729–732. **doi:10.1038/351729a0**

Troedson, A.L., and Davies, P.J., 2001. Contrasting facies patterns in subtropical and temperate continental slope sediments: inferences from east Australian late Quaternary records. *Mar. Geol.,* 172(3–4):265–285. **doi:10.1016/S0025-3227(00)00132-8**

Wyllie, M.R.J., Gregory, A.R., and Gardner, G.H.F., 1958. An experimental investigation of factors affecting elastic wave velocities in porous media. *Geophysics,* 23:459–493.

Zhang, L., Chan, L.-H., and Gieskes, J.M., 1998. Lithium isotope geochemistry of pore waters from Ocean Drilling Program Sites 918 and 919, Irminger Basin. *Geochim. Cosmochim. Acta,* 62(14):2437–2450. **doi:10.1016/S0016-7037(98)00178-1**

Zinke, J., Pfeiffer, M., Davies, G.R., Dullo, W.-C., and Camoin, G.F., 2005. First evidence of mid-Holocene and last interglacial seasonality in the tropical western Indian Ocean from corals [European Geosciences Union General Assembly 2005, Vienna, 24–29 April 2005].

Table T1. Expedition 310 coring summary.

Hole	Number of cores	Cored (m)	Recovered (m)	Recovery (%)
M0005A	12	16.35	5.37	32.84
M0005B	8	12.35	9.24	74.82
M0005C	16	27.91	14.81	53.06
M0005D	36	79.17	51.35	64.86
M0005E	4	2	1.6	80.00
M0006A	4	2	1.55	77.50
M0007A	36	44.4	30.74	69.23
M0007B	36	47.93	27.02	56.37
M0007C	22	30.75	11.13	36.20
M0008A	19	38.7	9.49	24.52
M0009A	18	21.54	9.29	43.13
M0009B	18	26.29	17.42	66.26
M0009C	21	24.41	12.66	51.86
M0009D	25	43.31	23.62	54.54
M0009E	12	19.4	14.11	72.73
M0010A	20	33.25	10.02	30.14
M0011A	12	16.08	7.89	49.07
M0012A	19	32.3	8.37	25.91
M0013A	5	9.55	1.1	11.52
M0014A	14	18.61	8.65	46.48
M0015A	41	41.08	29.87	72.71
M0015B	38	40.12	28.83	71.86
M0016A	36	37.91	21.58	56.92
M0016B	24	27.62	14.31	51.81
M0017A	21	40.56	22.94	56.56
M0018A	22	40.05	24.63	61.50
M0019A	34	65.81	27.06	41.12
M0020A	25	41.83	29.47	70.45
M0021A	22	33.58	25.14	74.87
M0021B	20	32.21	21.12	65.57
M0022A	4	7.7	4.4	57.14
M0023A	16	31.36	24.21	77.20
M0023B	16	31.12	21.13	67.90
M0024A	16	31.85	26.67	83.74
M0025A	13	20.33	15.09	74.23
M0025B	13	19.4	13.81	71.19
M0026A	8	11	6.43	58.45
Totals:	726	1099.83	632.12	57.47

Table T2. Location of description and measurements made during Expedition 310.

Shipboard *Hunter,* offshore Tahiti	Onshore Science Party, Bremen
Core description: • Core catcher description	Core description: • Split-core visual core description
Core photography: • Core catcher photography	Core photography: • Full-core and close-up photography
Whole-core multisensor core logging: • Density • Velocity • Magnetic susceptibility • Electrical resistivity	Discrete sample index physical properties: • Compressional *P*-wave velocity • Bulk, dry, and grain density • Water content • Porosity and void ratio
Inorganic geochemistry: • pH • Alkalinity • Ammonia concentration chlorinity	Inorganic geochemistry: • Dissolved cations • Bromide, chloride, and sulfate • Dissolved phosphate • Chlorinity
Microbiology: • Activity testing by ATP monitoring • Exoenzymes activity • Microscopy (DAPI staining)	Microbiology*: • SEM analysis (including SEM-EDAX analysis) • Cultivation of microorganisms • Culturing
Downhole logging • Optical imaging • Acoustic imaging • Borehole fluid temperature and pressure • Electrical conductivity • pH • Oxydo-reduction potential (Eh) • Spectral natural gamma ray • Induction resistivity • Full waveform sonic • Caliper	Other: • Thermal conductivity (where possible) • Color reflectance of split-core surface at discrete points • Continuous digital line-scanning of split-core surface • X-ray fluorescence (14 samples from Hole M0008A)

Note: * = Analyses conducted at the Swiss Federal Institute of Technology (ETH) Zurich, Switzerland, between the end of the offshore phase and the beginning of the Onshore Science Party. ATP = adenosine triphosphate, DAPI = 4′,6-diamindino-2-phenylindole, SEM = scanning electron microscopy, EDAX = X-ray energy dispersive analyzer.

Table T3. Major and trace element analyses of representative volcaniclastic sediments.

	310-M0008A-													
Core, section, Interval (cm):	4R-1, 22–28	5R-1, 15–20	7R-CC, 4–13	8R-1, 42–51	8R-1, 61–80	9R-CC, 0–5	10R-1, 27–30	14R-1, 0–10	14R-1, 24–28	16R-1, 55–60	16R-1, 115–120	17R-1, 0–5	17R-1 10–15	17R-1 18–23
Description:	Gray sand/silt	Gray sand/silt	Boulder 1	Boulder 2	Cobble	Pebble	Pebble	Pebble	Brown sand/silt	Brown sand/silt	Brown clay/sand	Pebble	Pebble	Pebble
Major element oxide (wt%):														
SiO_2	32.79	29.86	42.15	42.68	42.32	41.01	37.80	44.03	41.44	38.90	31.37	43.59	45.15	47.06
TiO_2	2.97	2.83	3.15	3.13	1.77	3.46	2.90	4.07	3.22	3.39	3.84	3.33	3.69	3.64
Al_2O_3	13.22	11.92	15.56	15.83	8.51	15.87	9.69	16.50	12.04	14.80	13.88	14.85	14.96	16.66
Fe_2O_3	13.02	12.13	12.16	12.26	10.84	12.38	12.90	10.33	15.78	16.05	16.59	12.18	11.68	11.39
MnO	0.15	0.14	0.16	0.17	0.17	0.18	0.17	0.13	0.16	0.21	0.36	0.15	0.16	0.16
MgO	9.99	9.67	4.98	6.04	16.76	4.33	14.22	3.07	4.96	5.15	2.95	5.59	4.48	5.08
CaO	7.63	9.12	9.58	9.98	12.02	8.96	9.12	8.89	1.36	1.60	1.44	9.37	7.63	9.98
K_2O	0.81	0.71	1.21	1.07	0.44	1.45	0.95	2.01	0.73	0.76	0.84	1.48	2.04	1.81
P_2O_5	0.30	0.26	0.69	0.66	0.14	0.51	0.25	0.90	0.05	0.23	0.32	0.58	0.88	0.88
Trace element (ppm):														
Sr	432	544	675	662	258	646	414	754	287	370	422	609	808	722
Ba	100	211	398	319	125	503	320	750	288	279	324	361	523	480
Rb	23.2	21.4	22.8	22.5	11.1	30.9	23.2	40.1	35.8	29.6	37.5	31.2	56.8	40.5
Cu	54.1	61.2	93.9	88.2	45.2	113	67.8	51.1	51.3	66.0	70.6	69.1	72.7	69.0
Ni	241	248	50.9	54.1	381	66.1	453	90.9	230	305	286	100	30.8	73.3
Zn	104	97.0	95.3	93.6	67.7	99.3	98.0	89.3	113	124	122	103	120	116
S	13,250	15,180	204	160	155	2,496	176	423	468	538	407	125	107	333
Cl	8,394	7,903	158	230	< 2.0	5,305	737	4,873	10,210	9,140	8,032	293	163	327
Br	24.6	19.7	1.1	1.6	< 1.4	10.3	< 1.6	10.9	37.1	29.7	28.4	1.0	< 1.7	< 1.8

Figure F1. Sea-level history reconstructed for long drill cores from Tahiti (squares), Barbados (circles), and New Guinea (triangles) (from Bard et al., 1996). Reconstructed sea-surface temperatures for various time windows on corals from the Vanuatu (Beck et al., 1997). MWP = meltwater pulse.

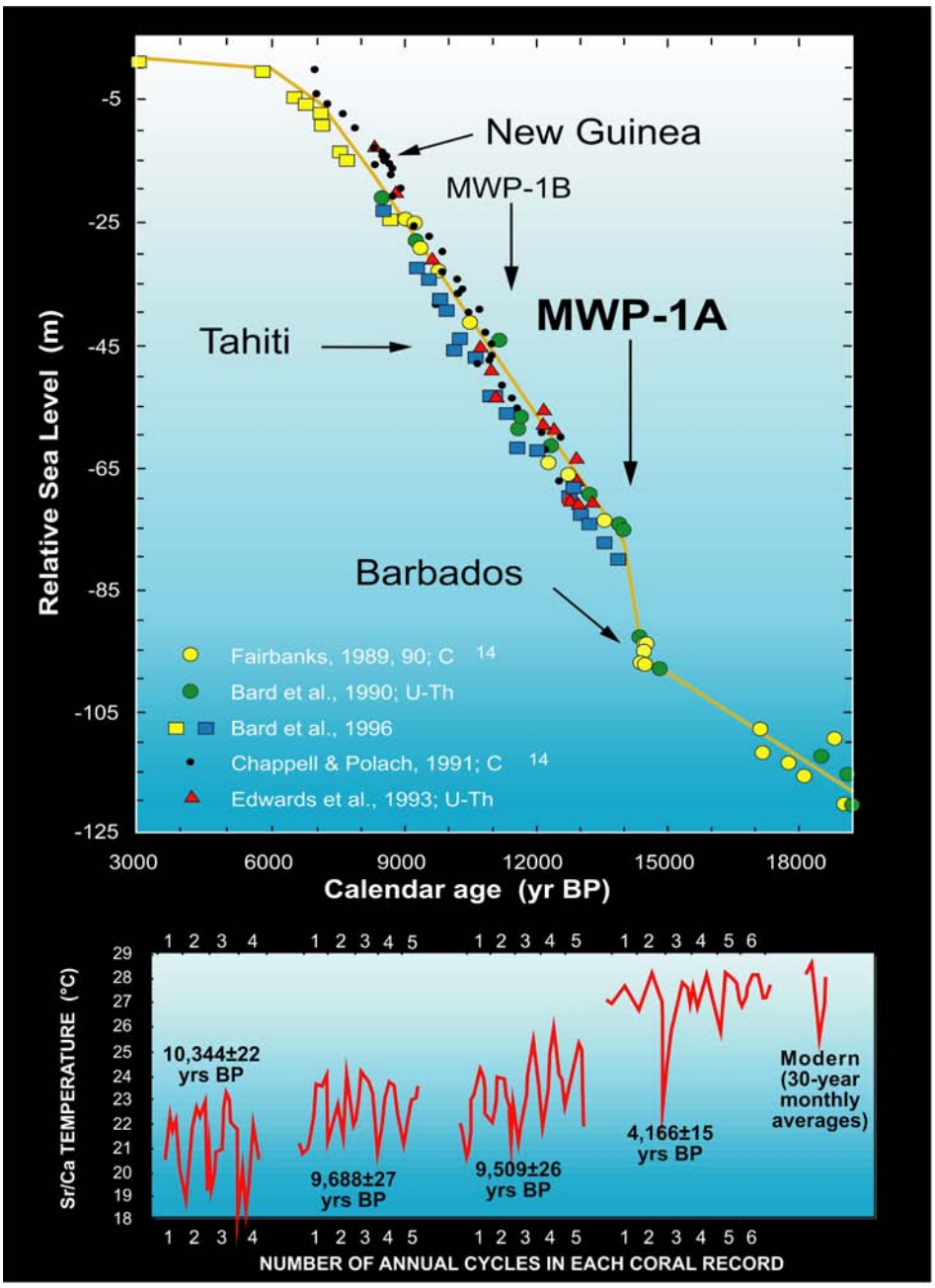

Figure F2. Location of Expedition 310 operations areas around Tahiti.

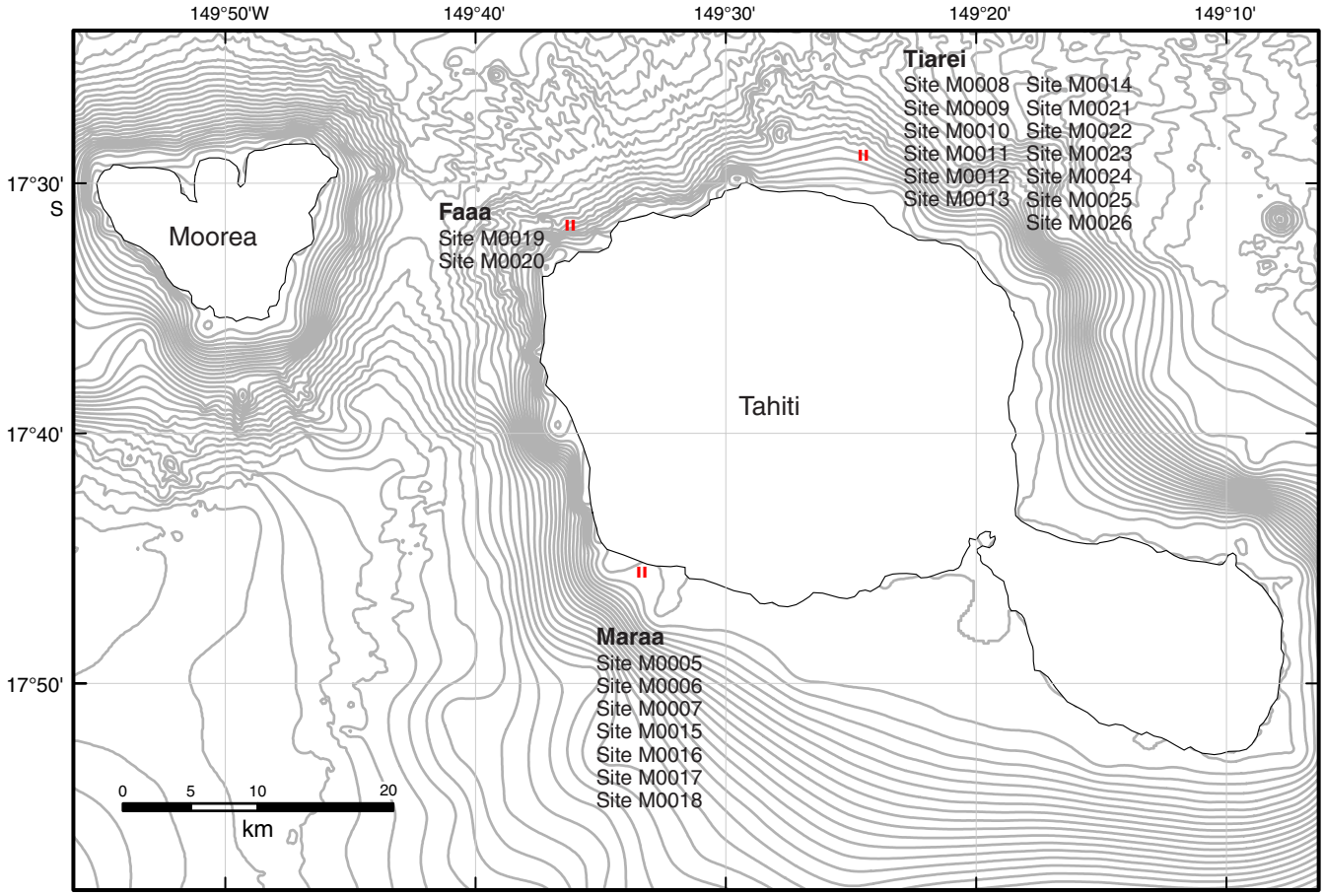

Figure F3. Location of Expedition 310 holes in the Faaa area (see Fig. **F2** for location with respect to Tahiti).

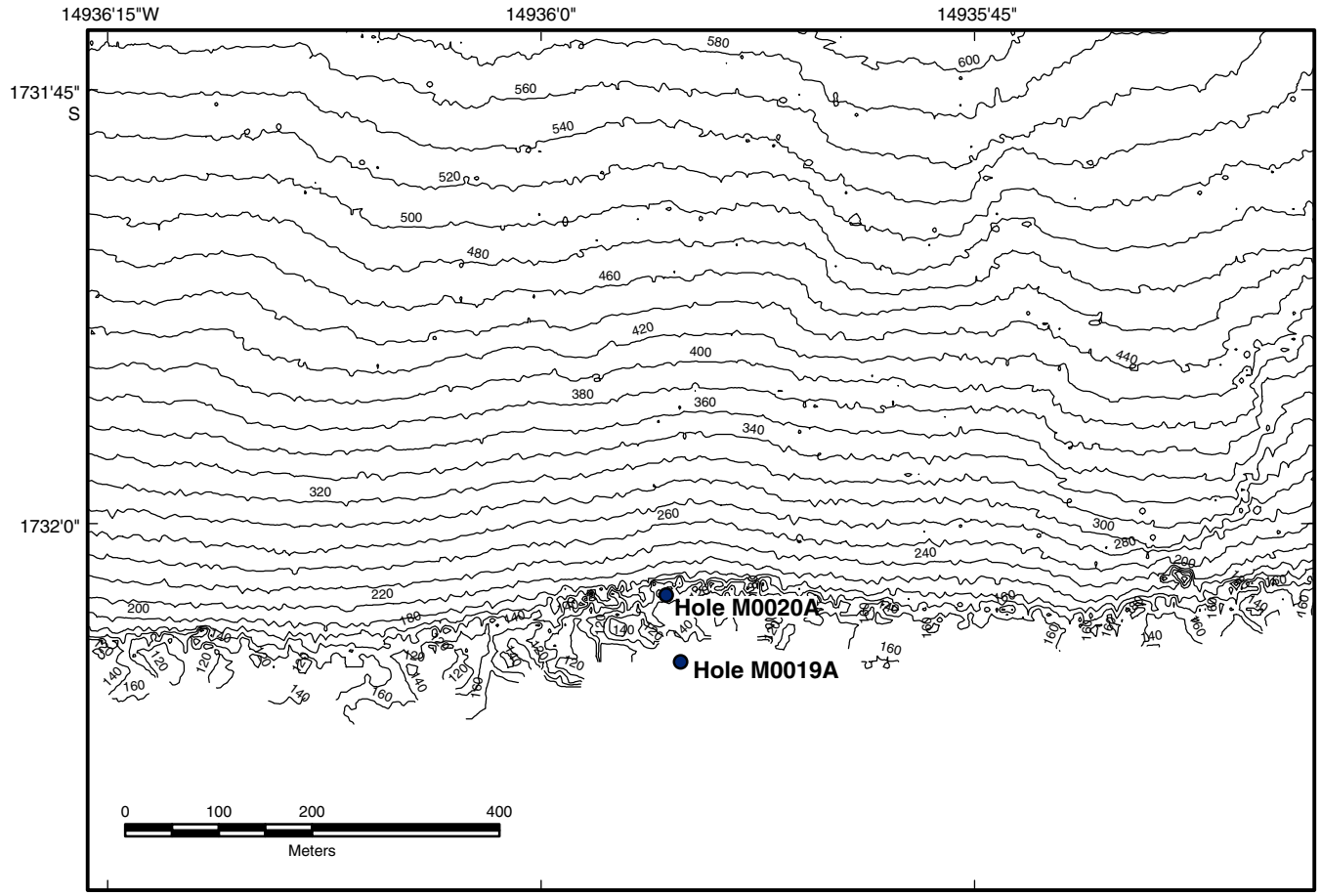

Figure F4. Location of Expedition 310 Holes in the Tiarei area (see Fig. **F2** for location with respect to Tahiti).

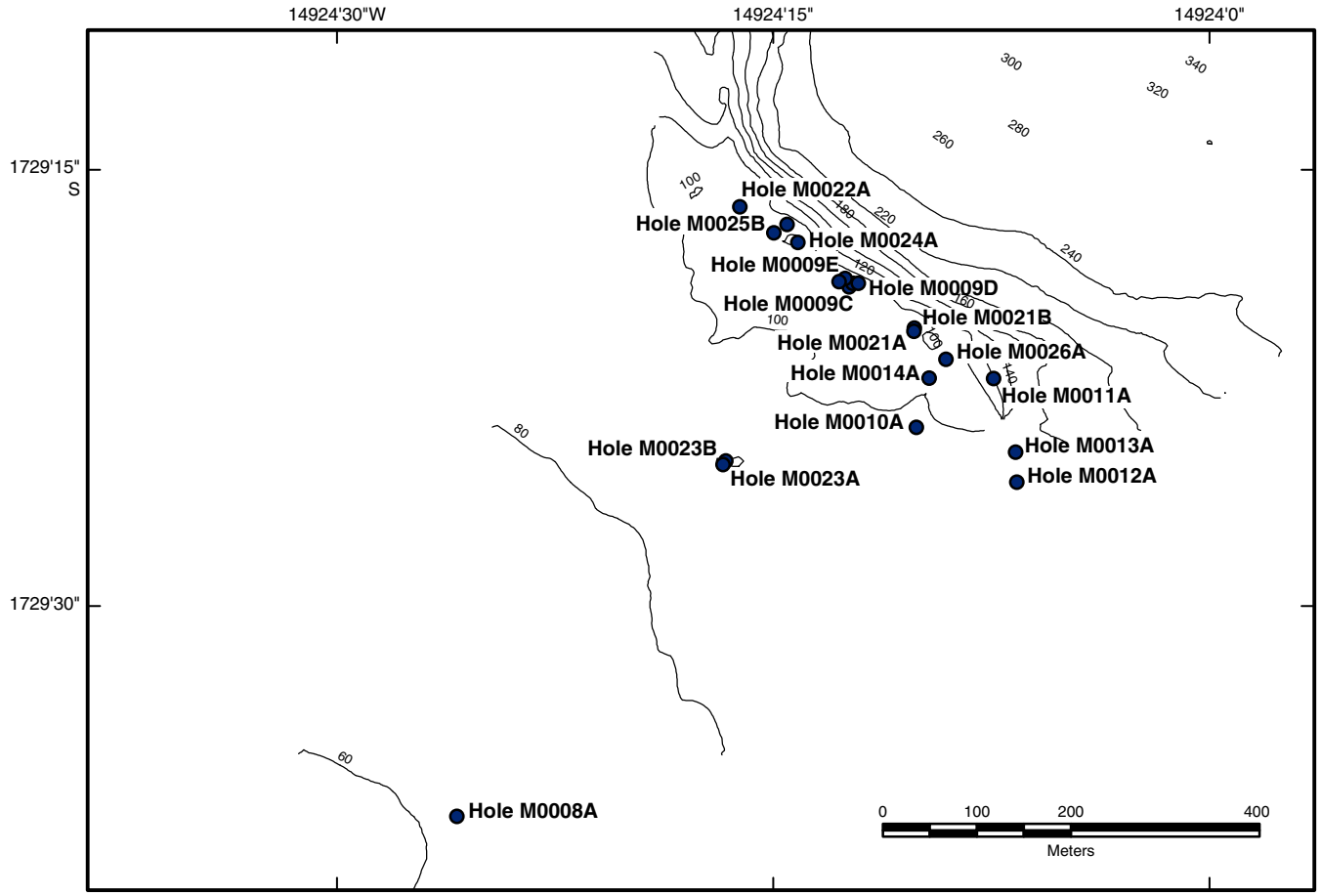

Figure F5. Location of Expedition 310 Holes in the Maraa area (see Fig. **F2** for location with respect to Tahiti).

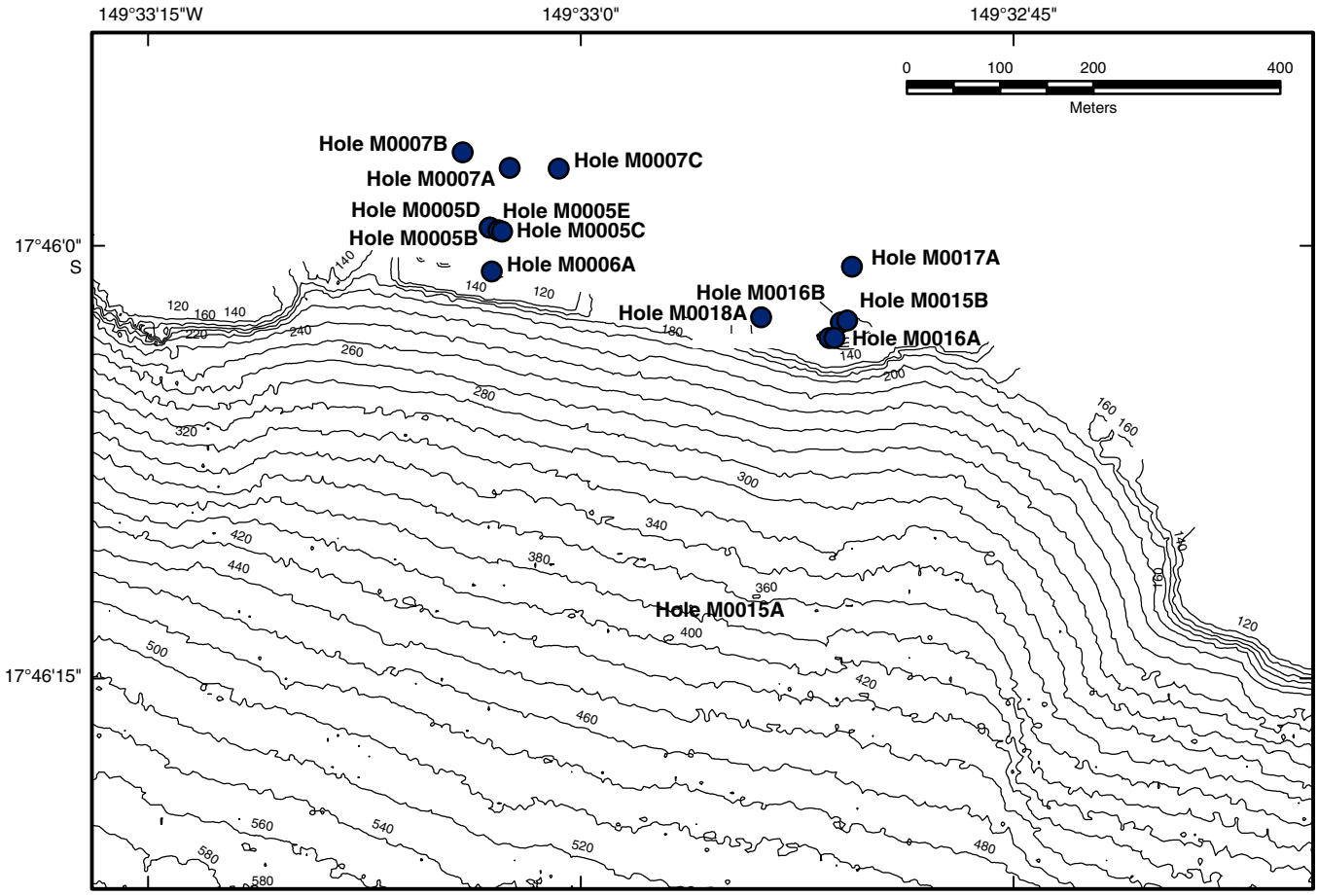

Figure F6. Lithostratigraphic summary of holes on the Maraa western transect. (Continued on next page.)

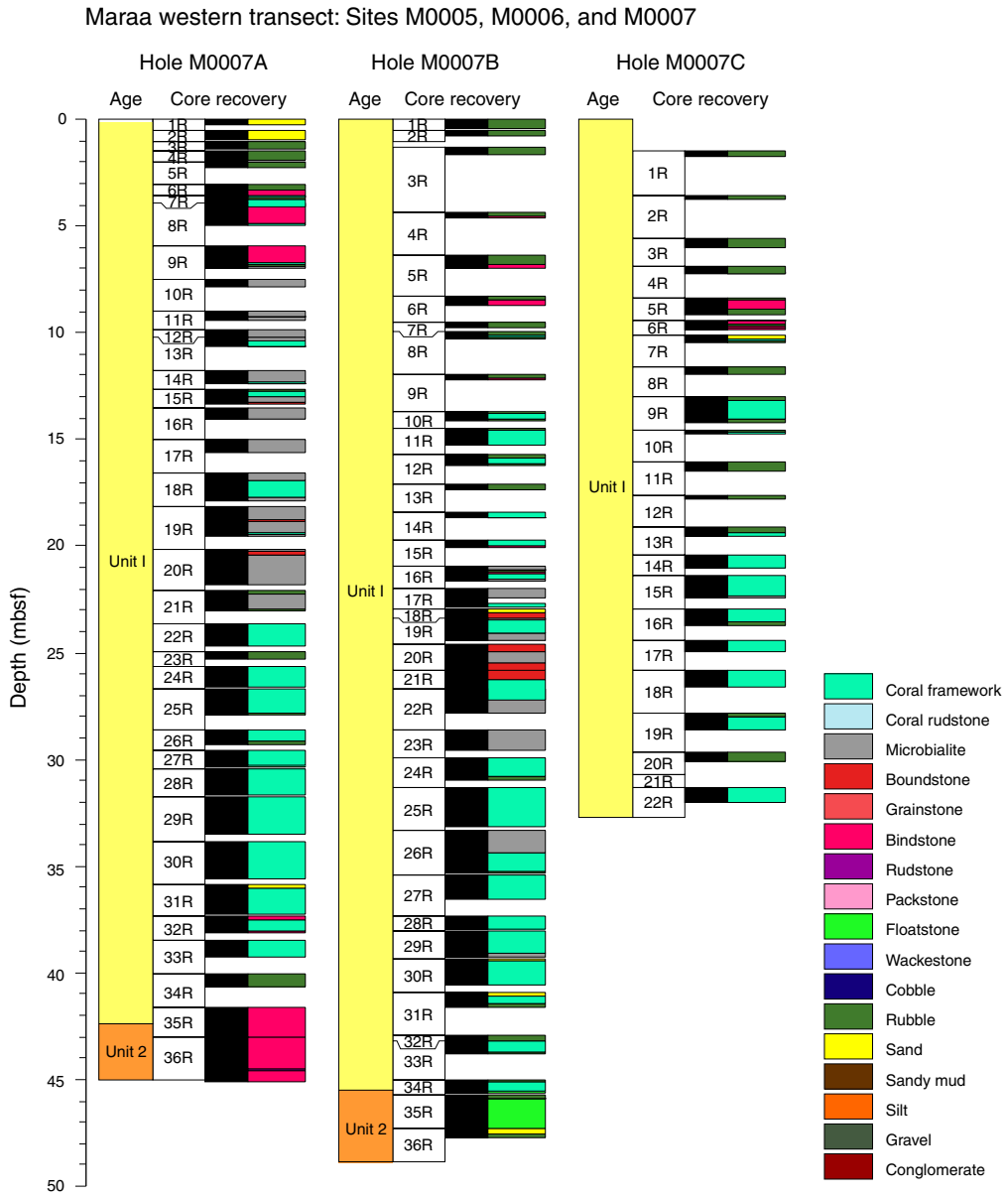

Figure F6 (continued).

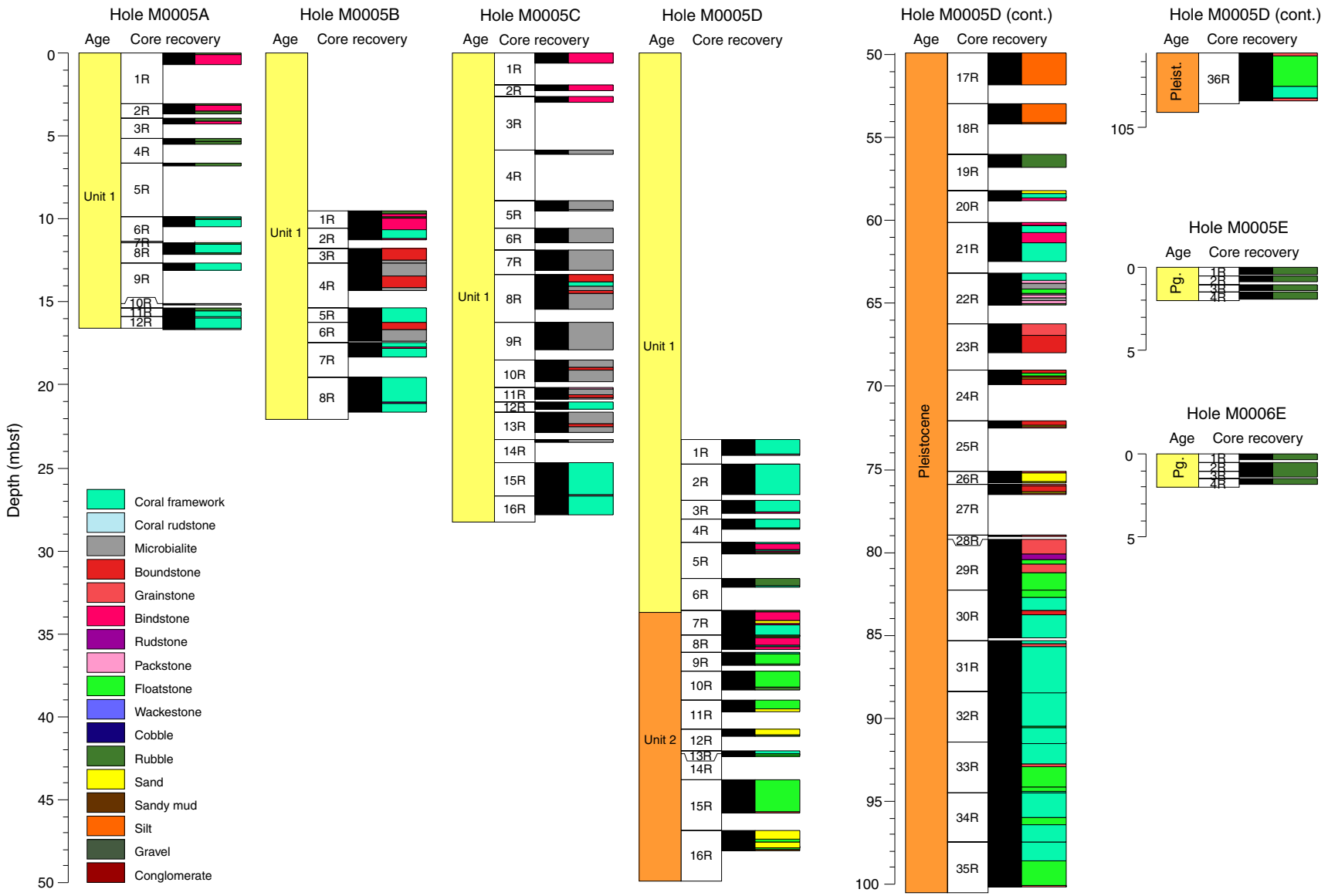

Figure F7. Lithostratigraphic summary of holes on the Maraa eastern transect.

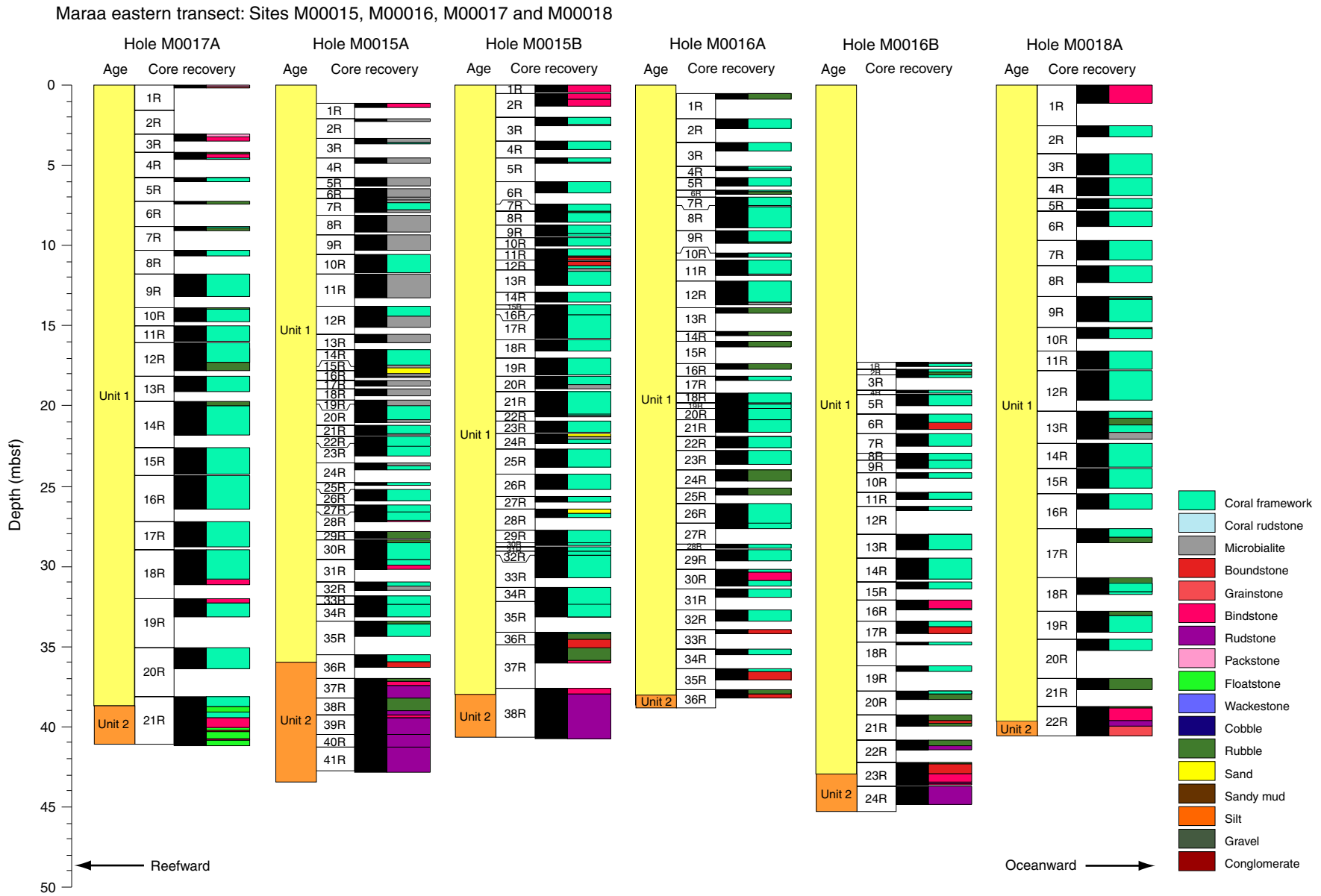

Figure F8. Lithostratigraphic summary of holes on the Tiarei inner ridge.

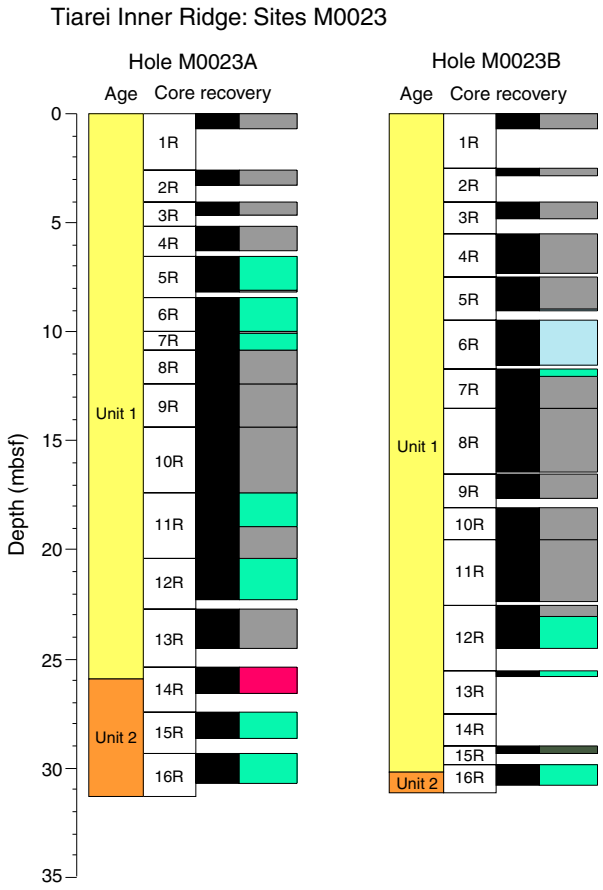

Figure F9. Lithostratigraphic summary of Holes on the Tiarei outer ridge. (Continued on next page.)

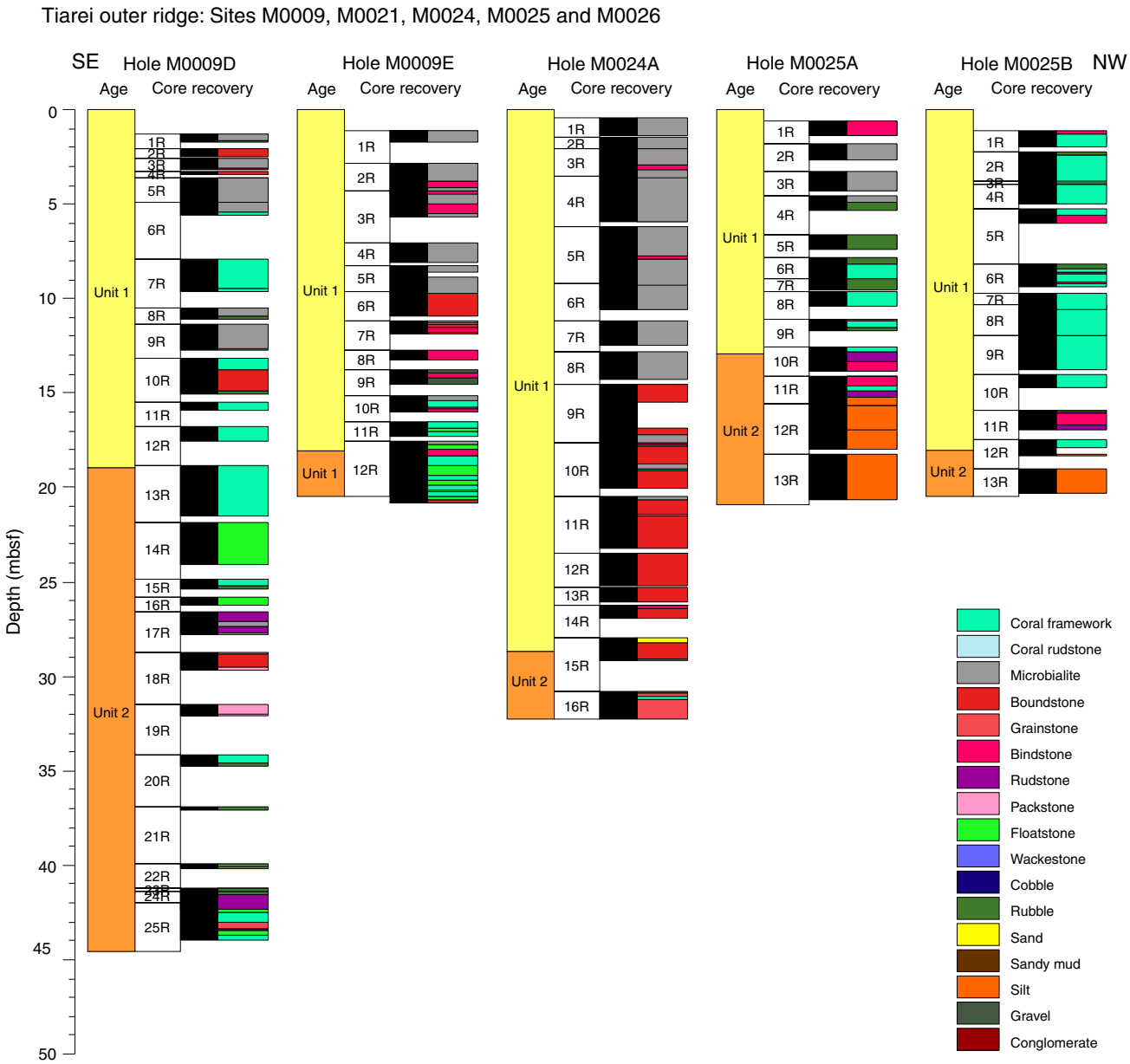

Figure F9 (continued).

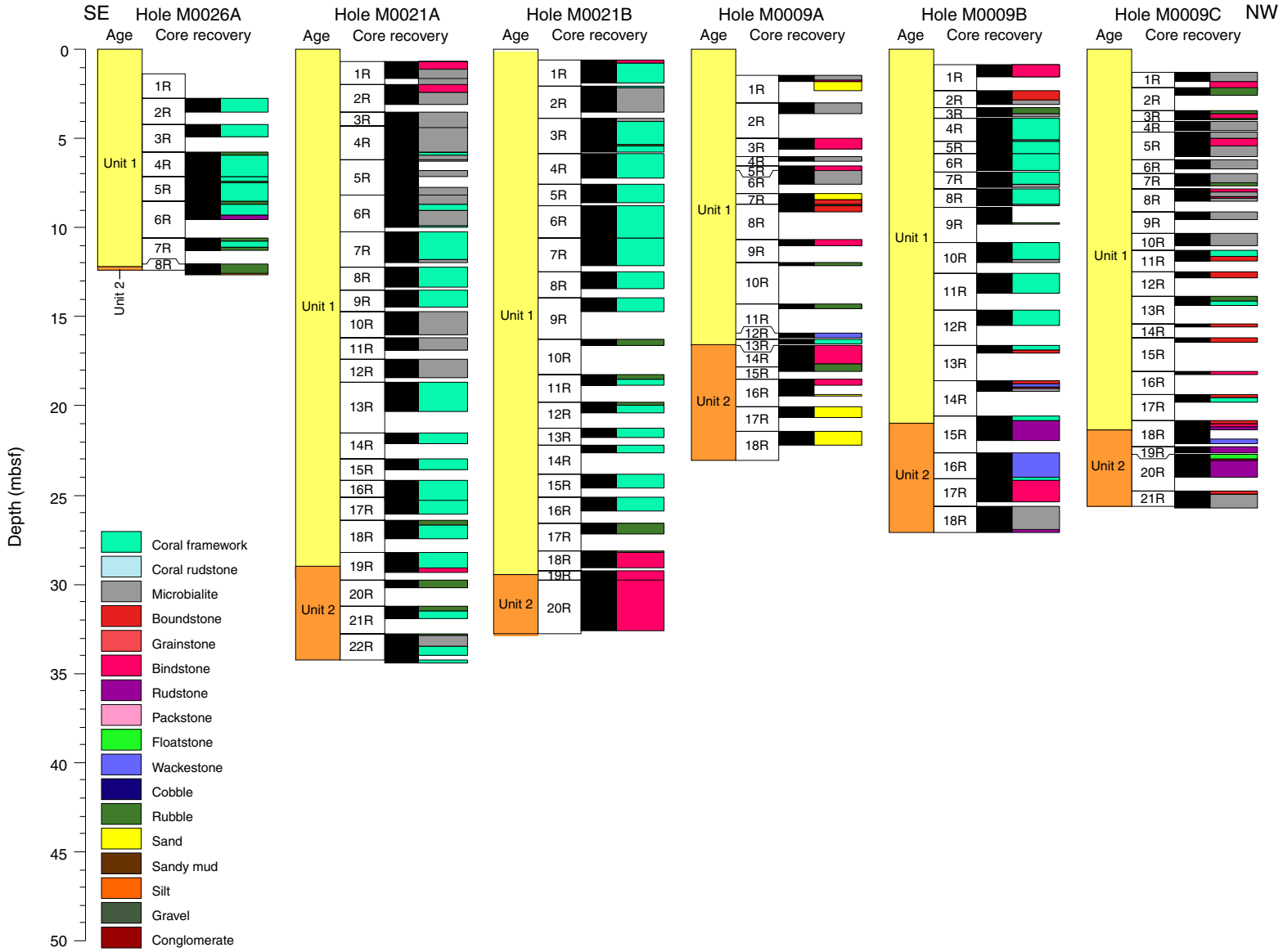

Figure F10. Lithostratigraphic summary of holes of the Tiarei marginal sites

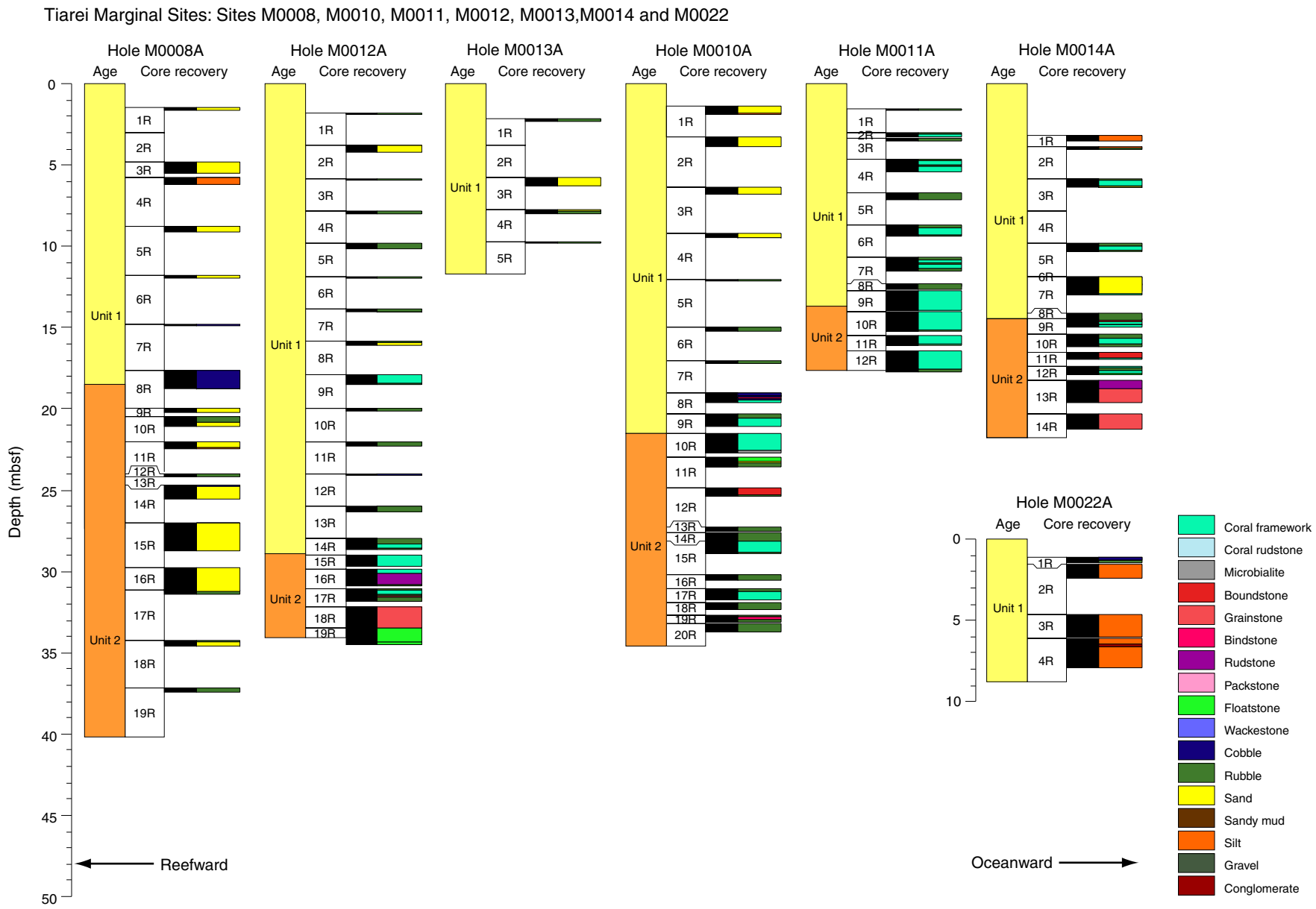

Figure F11. Lithostratigraphic summary of holes in the Faaa area.

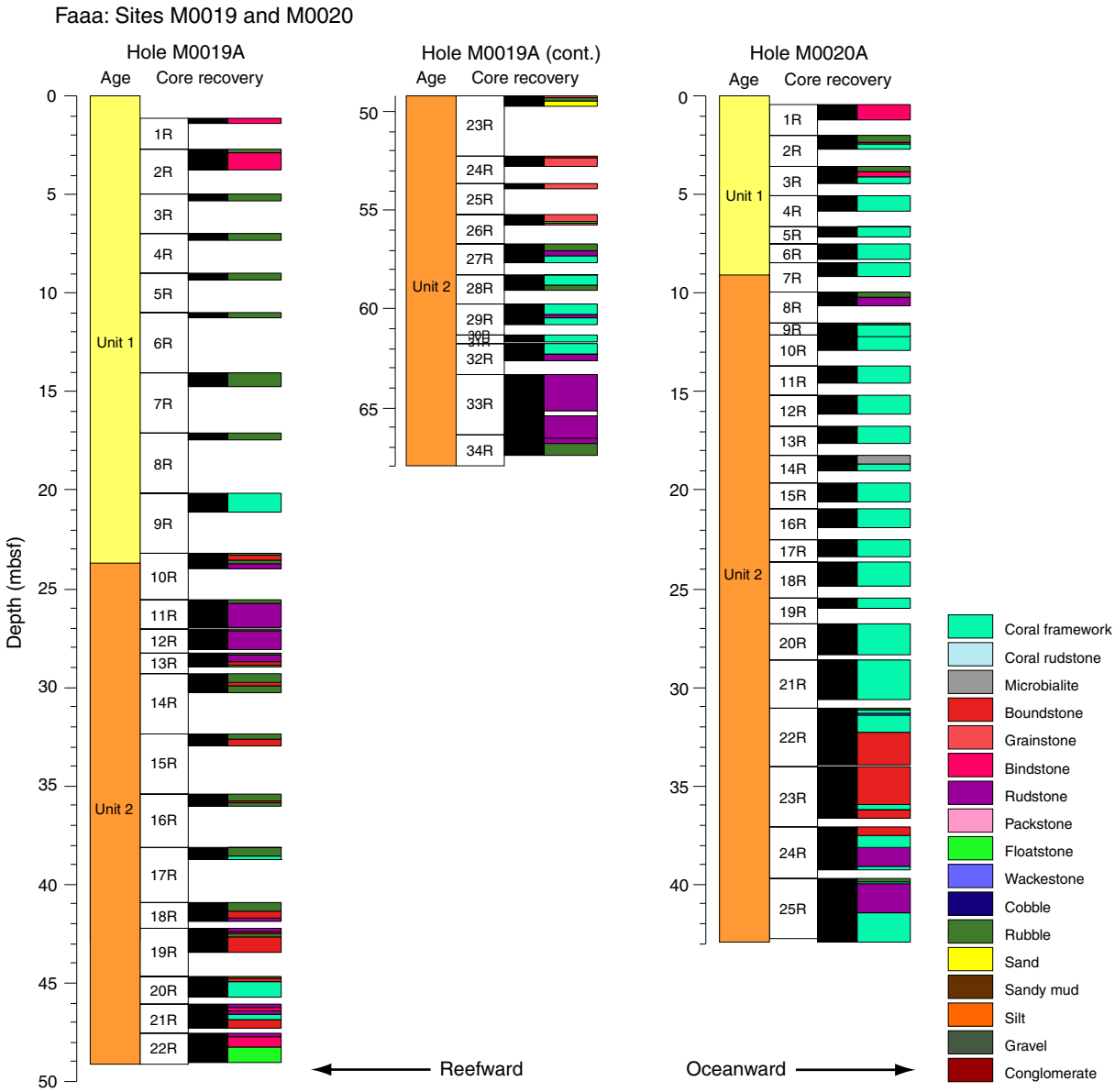

Figure F12. Cross plot showing all physical property data in the porosity and *P*-wave velocity domain. Instead of showing individual data points for the bulky MSCL data (15,191 data points), data density was contoured by moving a bin size of 0.200 km/s by 0.02 porosity units diagonally with increments of 1/30 of one bin size. Data density increases from blue to red. Purple = discrete sample properties (N = 355). In addition, commonly used velocity transforms, like those by Raymer (1980) and Wyllie (1956), are superimposed.

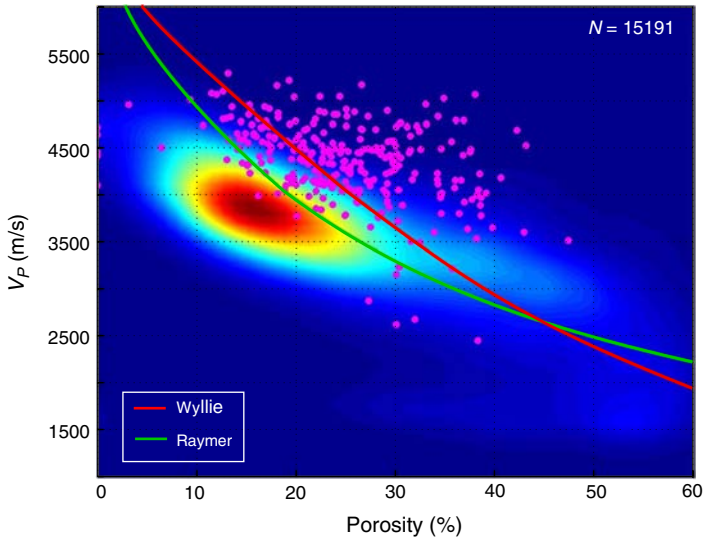

Figure F13. Composite of optical image (OBI), acoustic image (ABI), and total gamma ray (TGR) downhole logging data for holes in the Tiarei area (see Fig. **F4** for locations).

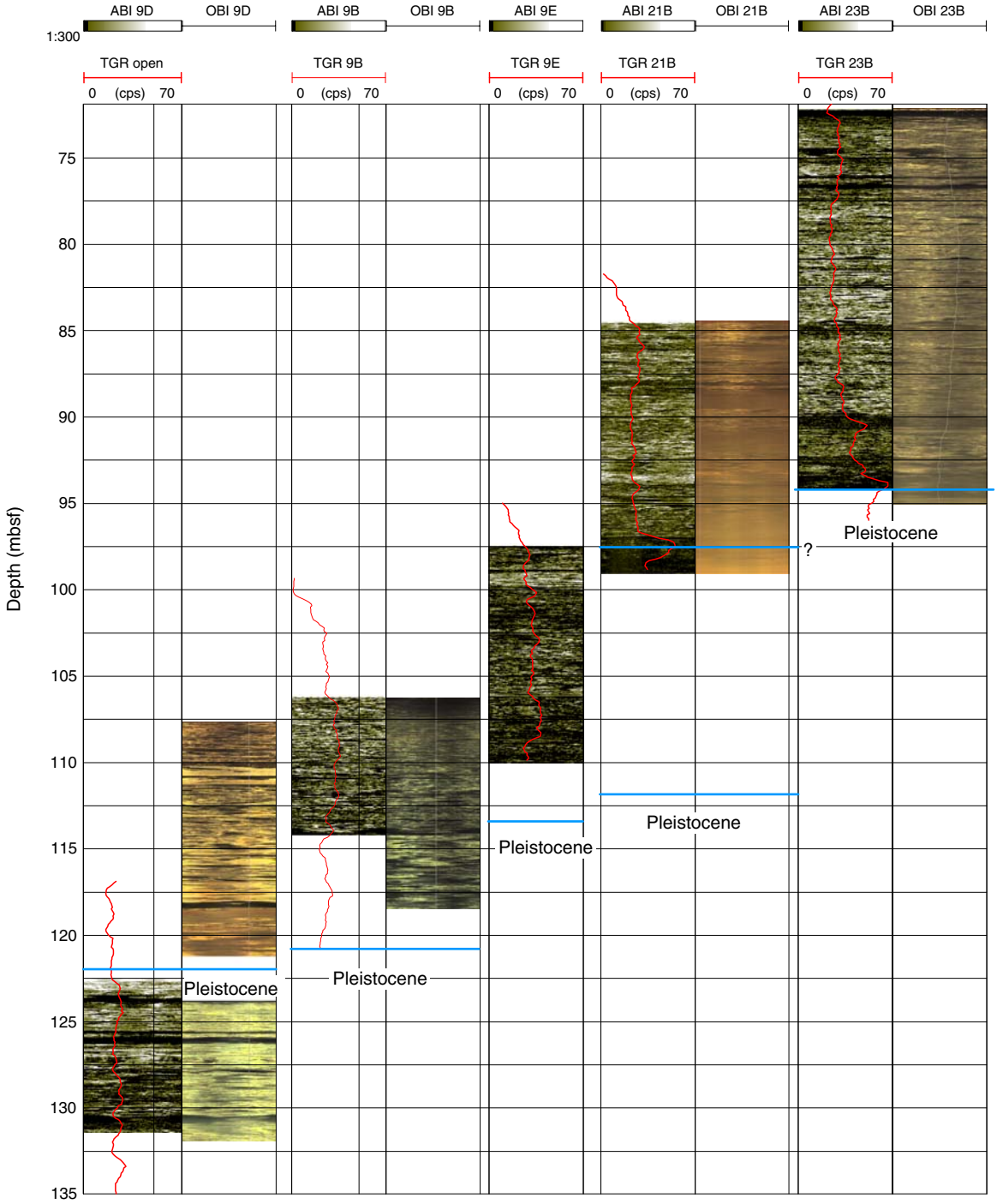

Figure F14. Composite of optical image (OBI), acoustic image (ABI), and resistivity downhole logging data for holes in the Tiarei area (see Fig. **F4** for locations). ILD = induction resistivity deeper investigation depth, ILM = induction resistivity medium investigation depth.

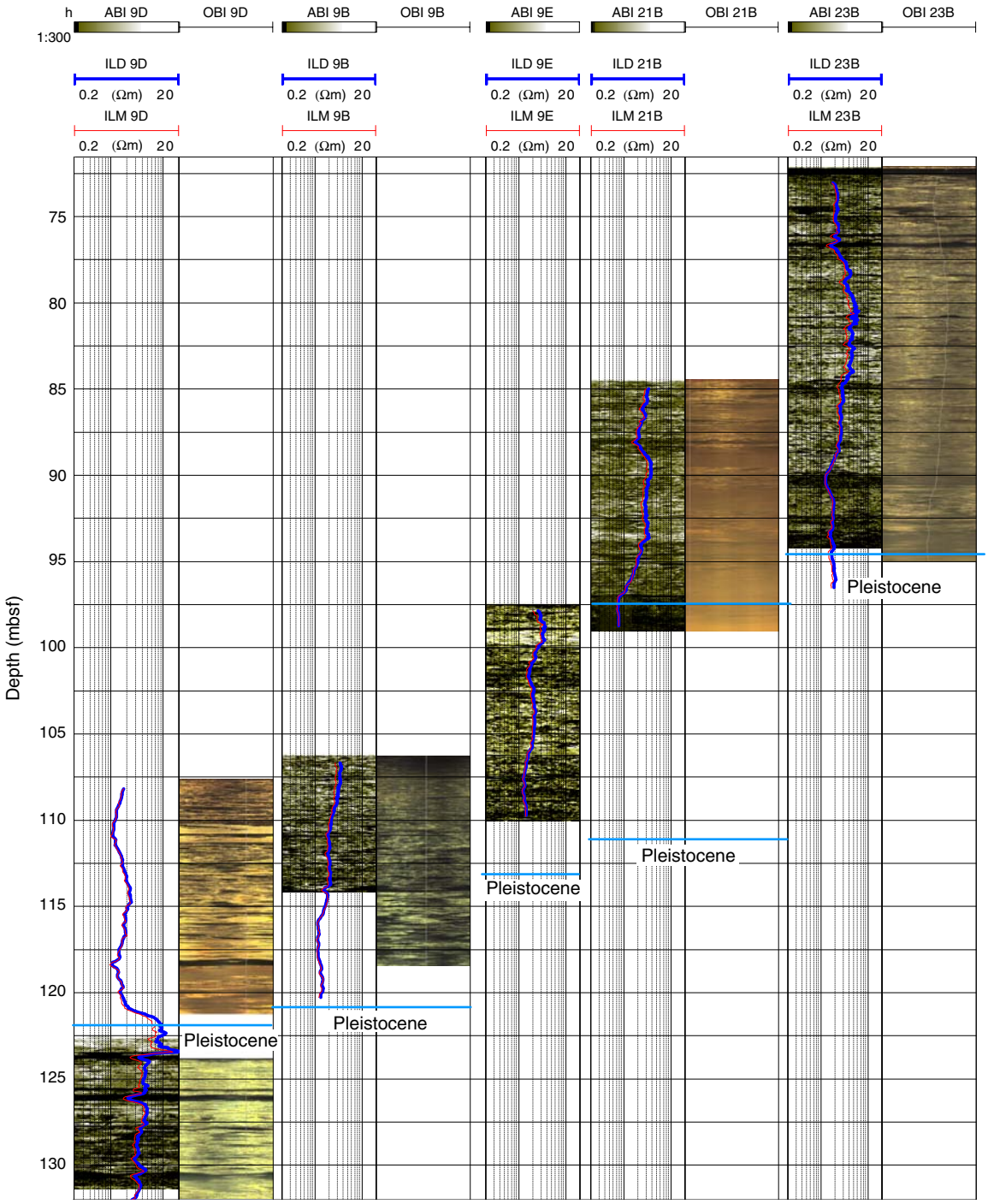

Figure F15. Composite of optical image (OBI), acoustic image (ABI), and total gamma ray (TGR), and resistivity downhole logging data for holes in the Maraa area (see Fig. **F5** for locations). ILD = induction resistivity deeper investigation depth, ILM = induction resistivity medium investigation depth.

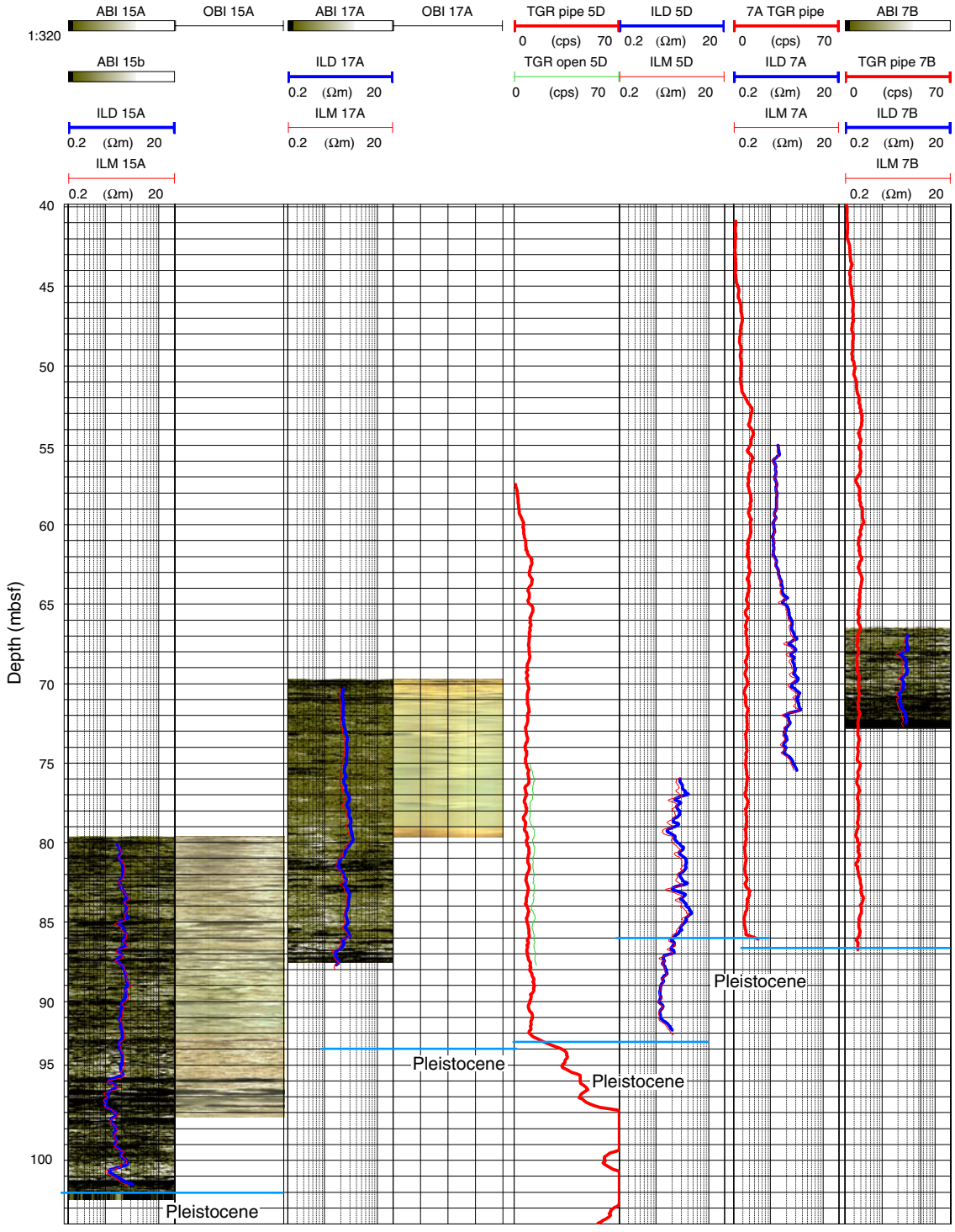

Figure F16. Brown iron/manganese crust and cavity (Hole M0016B; 23.68 mbsf).

Figure F17. Blue/purple biofilm with high microbial activity and high abundance of cells (Hole M0015B; 0.47 mbsf).

Figure F18. High abundance of cells in a biofilm (Hole M0015B; 0.47 mbsf; DAPI-stained fluorescence microscopy).

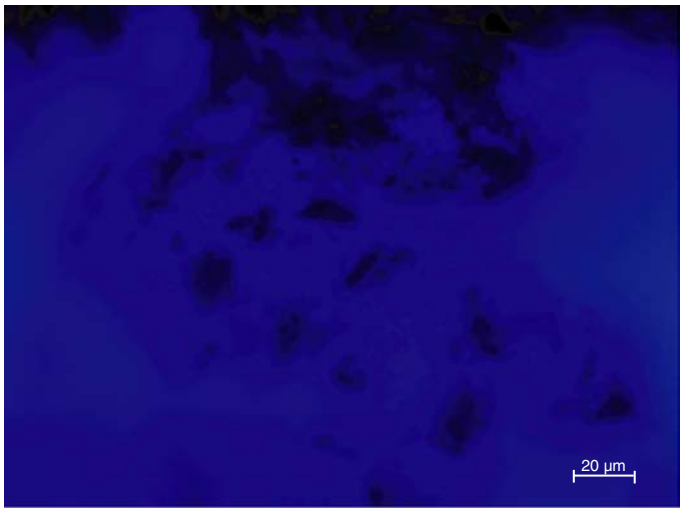

Figure F19. Surface of microbialites with some fiber type minerals, most probably clay minerals (Hole M0007C; 5.88 mbsf; glutaraldehyde fixed SEM at 30,000×).

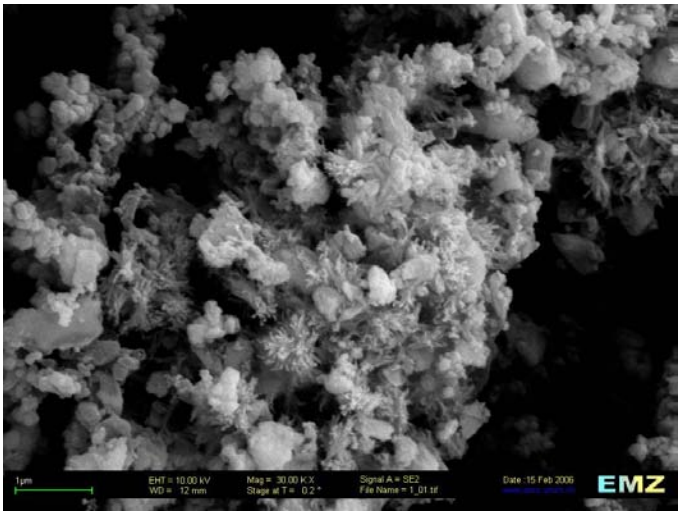

Figure F20. Surface of blue biofilm covered with a network of desiccated exopolymeric substances, minerals, probably carbonates, and microorganisms (Hole M0015B; 0.47 mbsf; glutaraldehyde fixed SEM at 19,200×).

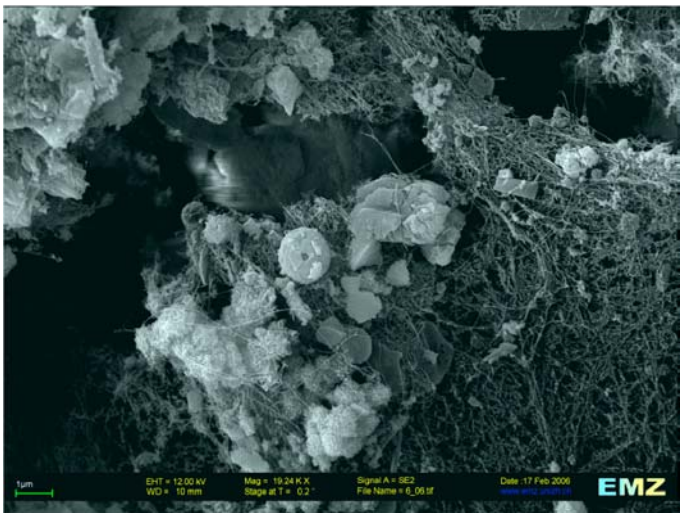

Figure F21. Surface of microbialites with framboidal pyrite crystals (Hole M0023A; 0.12 mbsf; glutaraldehyde fixed SEM at 9550×).

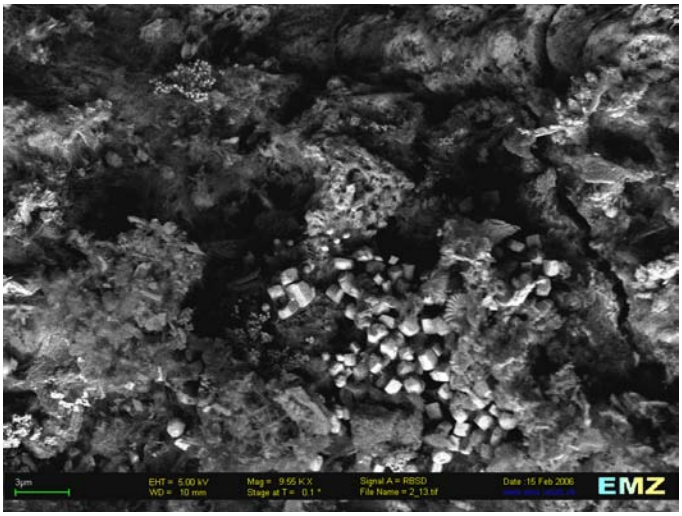

Figure F22. Aerobic pure cultures of microorganisms. The different colors originate from the different pigmentation by carotenoids.

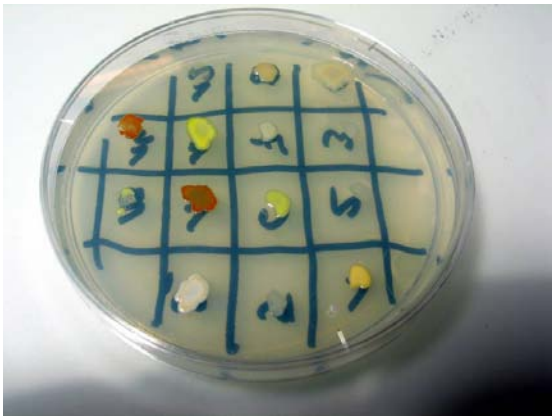

Figure F23. Rather high diversity of cell morphologies. Cells were common in this sample (Hole M0007C; 5.88 mbsf; DAPI-stained fluorescence microscopy).

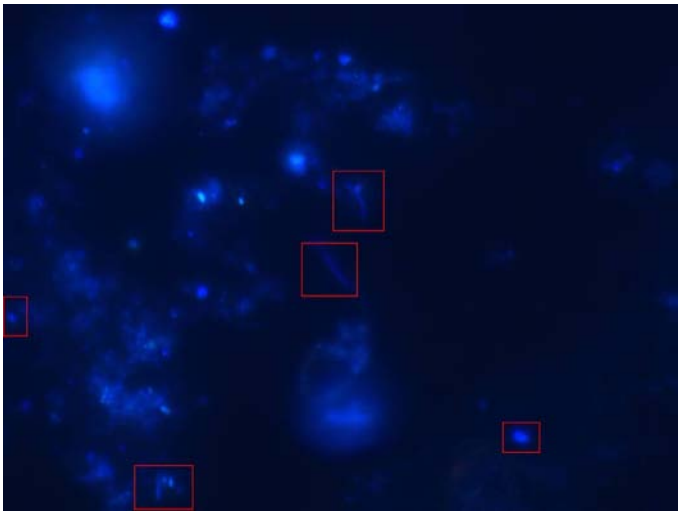

Figure F24. Interstitial water chemistry for Hole M0008A, showing depth profiles for (**A**) pH, (**B**) alkalinity, (**C**) ammonia, (**D**) potassium, (**E**) calcium, (**F**) strontium), (**G**) manganese, and (**H**) iron.

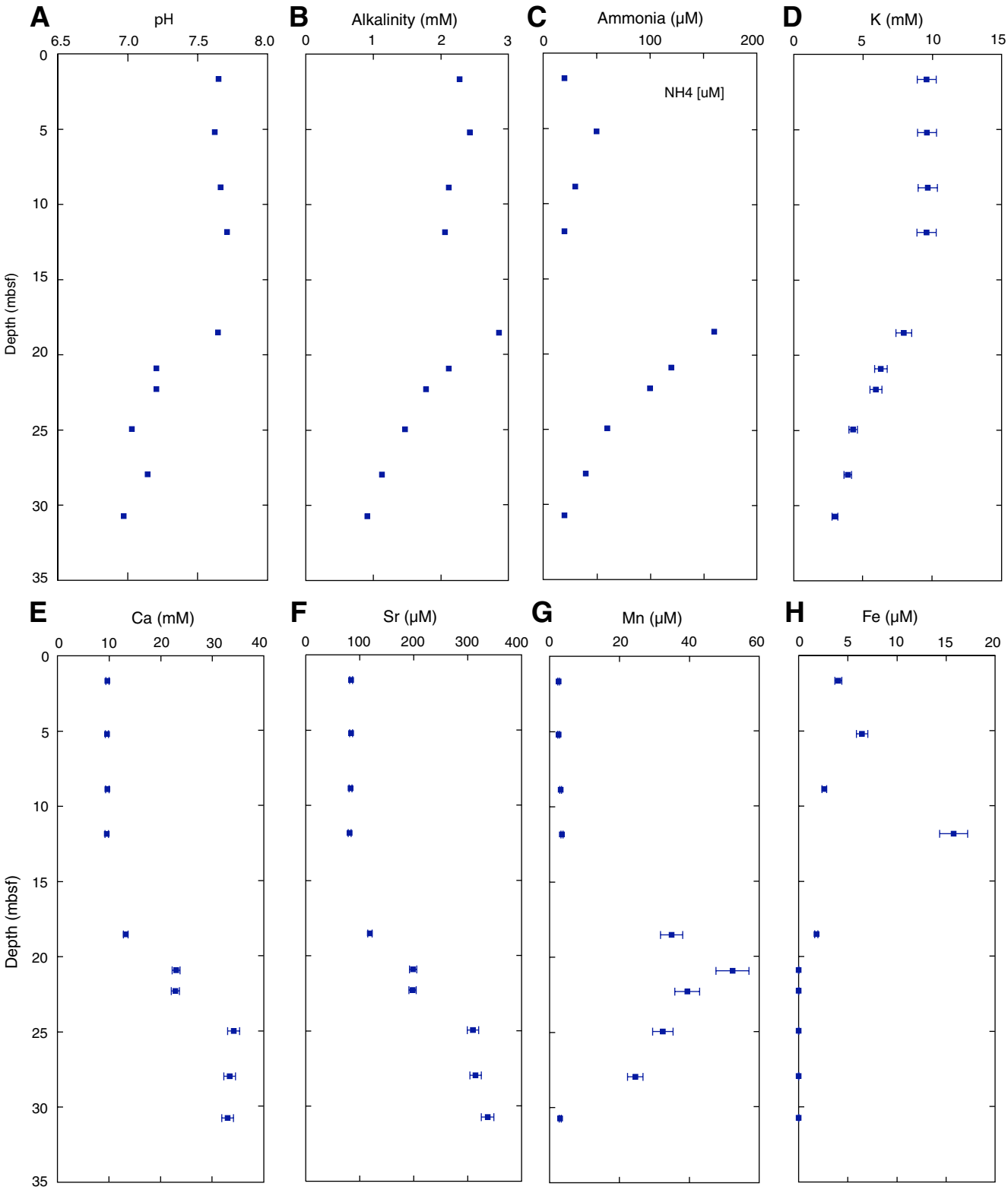

Figure F25. (**A**) SiO_2, (**B**) K_2O, (**C**) Rb for whole-rock samples from Hole M0008A. Note the systematic increase in values with depth.

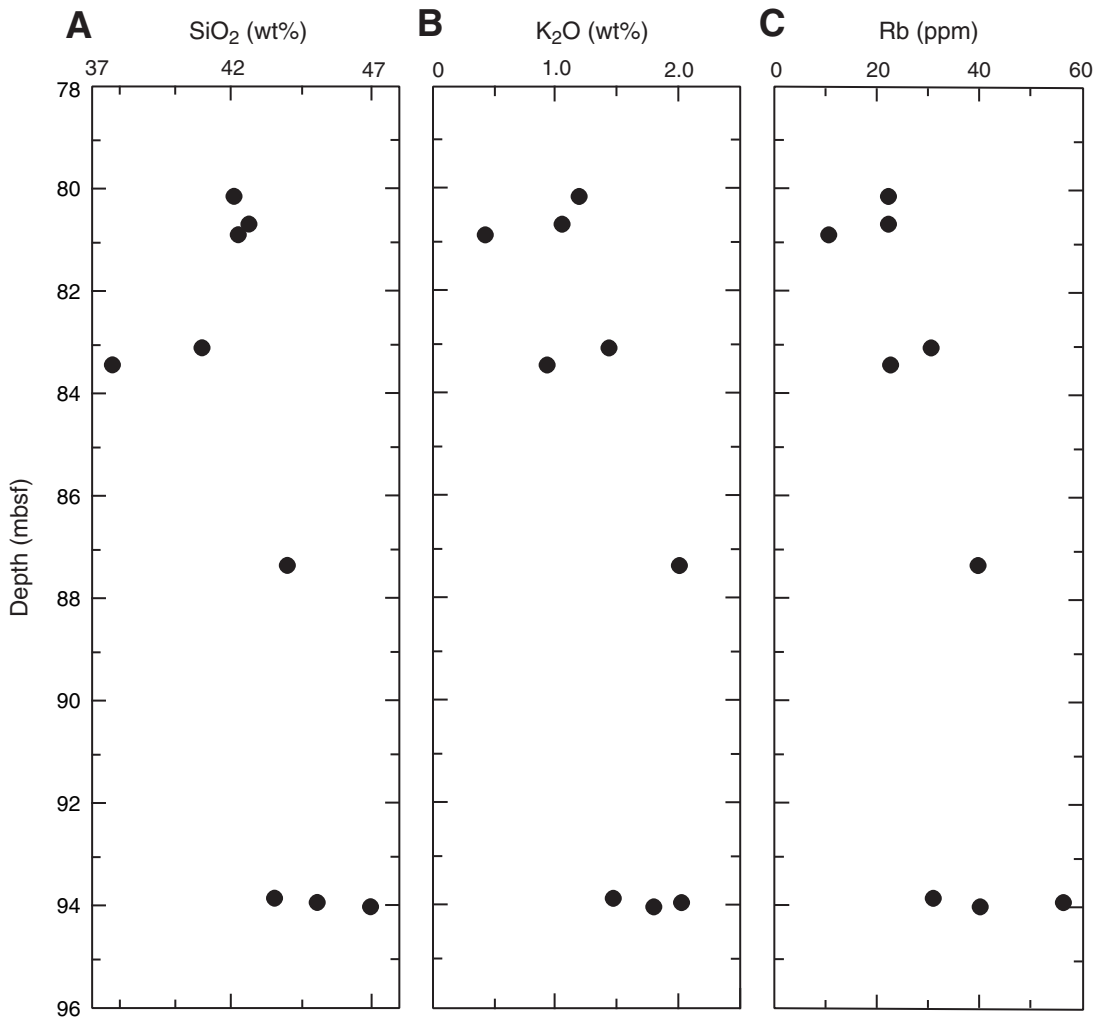

Figure F26. (**A**) CaO, (**B**) total Fe as FeO*, and (**C**) Rb volcanic sand/silt samples from Hole M0008A. Solid squares = upper gray unit, open squares = lower orange and brown units.

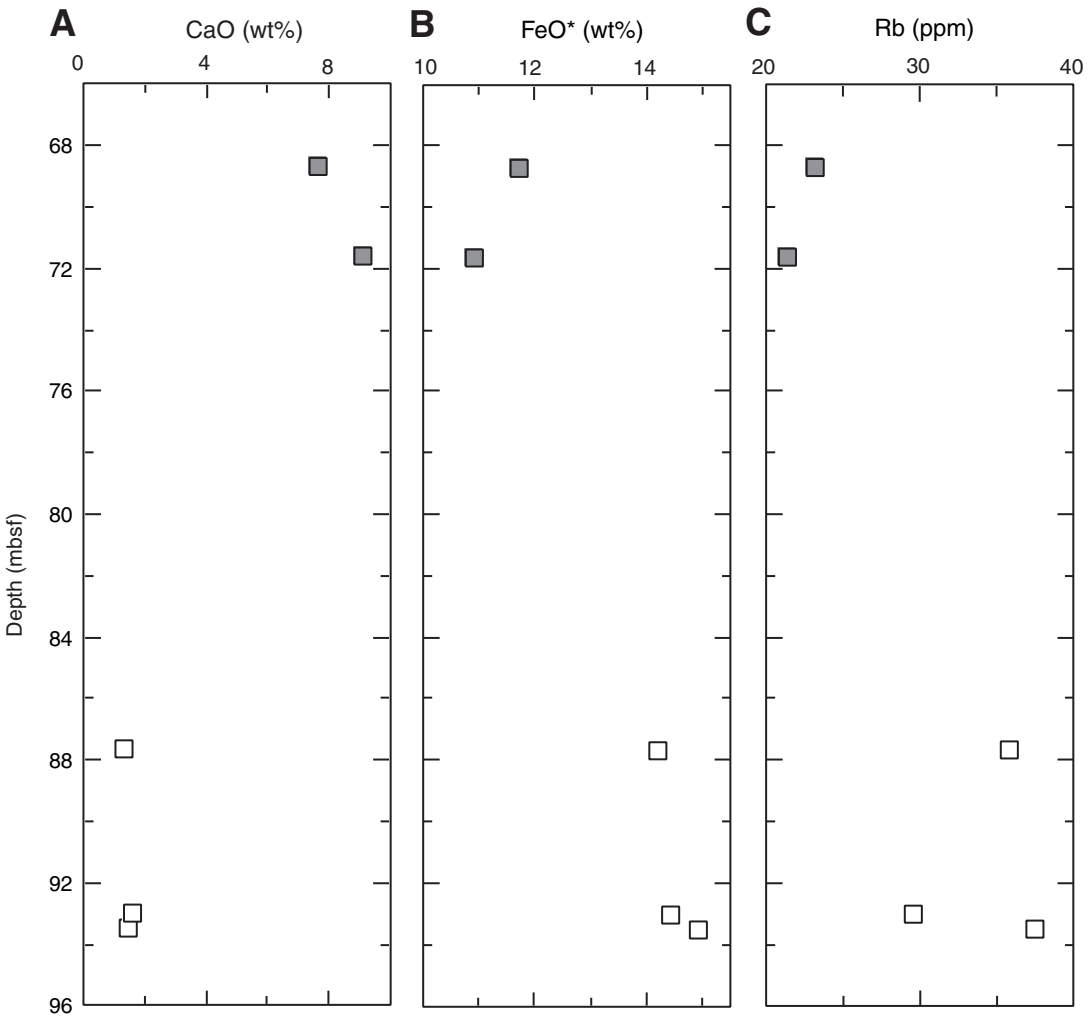

Figure F27. MgO versus (**A**) total Fe as FeO*, (**B**) K_2O, and (**C**) SiO_2 for whole-rock and volcanic sand/silt samples from Hole M0008A. Almost all the rock and gray volcanic sand/silt samples plot inside the Tahiti volcanic rock field, but the orange volcanic sand/silt samples plot farther away from the field, or in the case of C, out of the diagram. The Society volcano field in C includes samples from Tahiti and other volcanoes that belong to the Society Islands volcanic chain. Dark solid and light dashed lines in A represent model fractionation lines showing the change in magma composition with ~80% crystallization of a parent magma at two different oxygen fugacities using the model of Nielsen (1990). The dark solid line is for higher oxygen fugacity. Background data and figures are from Duncan et al. (1994) and Devey et al. (2003)